Università degli Studi di Firenze

DIPARTIMENTO DI MECCANICA E TECNOLOGIE INDUSTRIALI

TESI DI DOTTORATO DI RICERCA IN PROGETTO E COSTRUZIONE DI MACCHINE

XXII CICLO

Dynamic analysis of a Formula SAE car

CANDIDATO:

ING. TOMMASO INNOCENTI

RELATORE:

PROF. ING. RENZO CAPITANI

CONTRORELATORE:

PROF. ING. MASSIMO GUIGGIANI

COORDINATORE DEL CORSO:

PROF. ING. MARCO PIERINI

- 2009 –

Il mondo è pieno di cose ovvie che nessuno si prende mai la cura di osservare
(Sherlock Holmes)

Abstract

The aim of this PhD thesis is to define a methodology to deeply analyze the dynamic and handling of a Formula SAE car, focusing the attention on the creation of a vehicle model able to simulate almost all the common maneuvers that the formula has to perform during a typical race. During the development of this work, two different models have been created: a 3 DOF one and a 15 DOF one. Both of them, built starting from the effective Formula SAE car geometric and inertial data, have been tested on common maneuvers and the results compared with the real car telemetry, to prove the efficiency and correct response of the simulator. Both the models gave interesting results, always demonstrating to give correct outputs, compared to real car or to commercial software.

Contents

Introduction to the thesis

The aim of this PhD thesis is to define a methodology to deeply analyze the dynamic and handling of a Formula SAE car, focusing the attention on the creation of a vehicle model able to simulate almost all the common maneuvers that the formula has to perform during a typical race. This task has been performed following two steps: the first one is a deep analysis of a Formula SAE car dynamic behavior and handling. The second is the creation of a set of easily to configure tools that could assist the Firenze Race Team during the development of the new cars, effectively decreasing the amount of time needed to simulate the car behavior on track. After many years of activity in the Formula SAE races, it was decided to build a vehicle model dedicated to our cars, directly build on their geometries, that could be quickly configured to give the designer a series of indications on its probable behavior on track.

The first part of the work is a brief revision of the basic concepts of vehicle dynamics, including the bicycle vehicle model and the model of vehicle with locked differential. Even if shortly presented, this phase resulted really important in order to understand what could be the best way to model a vehicle and what hypothesis have to be introduced without paying them excessively during simulations.

In the second part, the model with three degrees of freedom is presented: the first model produced is able to accelerate the rear wheels using the engine torque and to turn, having variable locking ratios for the differential. In a first phase the model has been tested having different differential configurations. Thanks to the way it's constructed, the model is able to simulate, with only small adjustments, different kind of drivelines, from a simple rigid axle to a completely customizable limited-slip differential (LSD).

In a second time, thanks to the customizable driveline, a confrontation of the behaviors of the car with the differential locking percentage variation is analyzed and a study of its influence is developed, in order of handling. The under and oversteer behavior of a Formula SAE car is analyzed as a function of differential typology and some suggestion on locking percentage are presented.

In this part the handling problems related to the control of a vehicle with an active differential are presented, discussing about the different locking rations in various driving conditions.

The third part of this work presents the 15 DOF model created for the Formula SAE car of the Firenze Race Team and all its possible uses. The model, differently from the 3 DOF one, includes a fully working suspension system, effectively modeling its response to road-tyre interaction. Even for this model the whole construction blocks are presented, as well as its validation, comparing it with a commonly used commercial software. This model, even if with different customizable parameters, resulted to be a really power simulating tool, showing all the most important handling parameters of a car and their variations with different configurations. It has to be noted that the 15 DOF model, thanks to the way it has been modeled, could be used in two different ways: a dynamic simulator, implementing different maneuvers, or a poster-rig simulator, effectively modeling the road surface on each tyre.

1 Introduction to Formula SAE

1.1 What is Formula SAE?

Formula SAE is a student design competition organized by the Society of Automotive Engineers (SAE, also known as SAE International). The concept behind Formula SAE is that a fictional manufacturing company has contracted a student design team to develop a small Formula-style race car. The prototype race car is to be evaluated for its potential as a production item. The target marketing group for the race car is the non-professional weekend autocross racer. Each student team designs, builds and tests a prototype based on a series of rules, whose purpose is both ensuring on-track safety (the cars are driven by the students themselves) and promoting clever problem solving.

The prototype race car is judged in a number of different events. The points schedule for most Formula SAE events is:

Event Name	Available points
Design event	150
Cost & Manufacturing Analysis event	100
Presentation event	75
Acceleration event	75
Skidpad event	50
Autocross event	150
Fuel economy event	100
Endurance event	300
TOTAL	**1000**

In addition to these events, various sponsors of the competition provide awards for superior design accomplishments. For example, best use of E-85 ethanol fuel, innovative use of electronics, recyclability, crash worthiness, and analytical approach to design are some of the awards available. At the beginning of the

competition, the vehicle is checked for rule compliance during the Technical Inspection. Its braking ability, rollover stability and noise levels are checked before the vehicle is allowed to compete in the dynamic events (Skidpad, Autocross, Acceleration, Endurance and Fuel Economy).

Formula SAE encompasses all aspects of a business including research, design, manufacturing, testing, developing, marketing, management, and fund raising; as a matter of facts this competition is globally involving a whole University, with all its faculties and students. Formula SAE is, in the end, the only university activity that takes students out of the class room and puts them directly in the real world.

Big companies, such as General Motors, Ford, Ferrari, Dallara and Airbus, can have staff interact with more than 1000 student engineers. Working in teams of anywhere between two and 30, these students have proved themselves to be capable of producing a functioning prototype vehicle.

Today, the competition has expanded and includes a number of spinoff events. Formula Student is a similar SAE-sanctioned event in the UK, as well as Formula SAE Australasia (Formula SAE-A) taking place in Australia. A Formula SAE West division is taking place in California and the Verein Deutscher Ingenieure (VDI) is holding the Formula Student Germany competition at Hockenheimring. The Associazione Tecnica dell'Automobile (ATA) is holding an official event in Italy since 2005: the great help from our Team was fundamental to help ATA start the competition and managing it over these years.

In the end Formula SAE is the first step that a student could do in the real world of motorsport, hoping to be part of it in its future professional life.

1.1.1 Formula SAE cars

Formula SAE cars could be really different one from each other. Thanks to a particularly free set of rules it is possible to design and produce cars with different ideas, engines, chassis and innovative solutions. As is possible to imagine there are some rules to comply to, but they are intended not to limit ideas and solutions, but to effectively ensure drivers safety. According to rules cars must be formula style (it means they have to be open wheeled and single driver), with some general dimensions (like minimum wheelbase, tracks, chassis dimensions, etc.) and material requirements imposed (but many variations could be done if a Safety Equivalence calculation is submitted to competitions judges). Most important thing is that cars weight is not regulated, so students could try to reduce it as much as they can.

Many car aspects are free, and many solutions could be adopted on the car, according to students ideas. No limitations on electronics, materials, shapes

and adopted technologies are present, so it's possible to see incredibly different cars on race tracks and it's possible to study many different solutions. For what concerns engines they must be four-stroke piston engine with a displacement not exceeding 610cc per cycle. Again, engines modifications are completely free, including overcharging.

Many different cars took part in a Formula SAE race and a myriad of solutions for common problems could be found on them. An example could be the chassis manufacturing, that easily represents this idea: every car has, of course, one but they are completely different one from each other for materials used, shape, weight, manufacturing and functionality. It's easy to see a monocoque carbon fiber chassis nearby a common steel space frame chassis or to see two monocoque made with different technologies or materials. Figure 1.1 shows some Formula SAE cars from different Teams: in clockwise order we have Firenze Race Team, Rennteam Stuttgart, Squadra Corse Politecnico di Torino and TUG Racing cars.

Figure 1.1 - Formula SAE cars

Being Formula SAE so free for what concerns rules, means that one of the most limiting aspects of designing a car is the team budget and access to production technologies. This means that "rich" teams are capable of realizing cars with expensive technologies or to have many hours of testing and, consequently, more reliable cars.

1.2 Firenze Race Team

As we all know, passion for motorsport is our life. It's the spring that pushes us not to sleep to build a car, not to give up until the race is ended. When, in 2000, a small group of students and researchers decided to try to participate to Formula Student in UK, they probably didn't know that they were starting a long lasting tradition. Formula Student started in 1998 in Leicester and it was growing fast, including much more teams every year: it was a good chance to prove that our University was as strong as the others and to give students the possibility to apply their studies on track.

Firenze Race Team (once known as Team V2) came to life in the first months of 2000 and started its activity of official Formula SAE team of the Università degli Studi di Firenze. The first year was spent searching partners and sponsors and, as a matter of facts, was useful to start the activity. Many technical sponsors approached the activity with enthusiasm and passion and gave the newly born team the help needed to start the adventure.

So, thanks to Ducati, Magneti Marelli, Bacci Romano & C., and some other proud sponsor it was possible to design the first car of the team and bring the project to the Formula Student competition for the Class 3: it was a success, with the first prize won for this class and a big injection of enthusiasm for the team.

The next year the first Firenze Race Team car came to life; it was called F2003-V2, Figure 1.2, and it represented a great success for a new team with few money and few support from its own university.

Figure 1.2 - F2003-V2

The next coming years were rich of successes and prizes and the team kept on his work, always building its cars with new solutions and ideas, but always facing budget problems and a lack of multidisciplinary quality (the whole team was composed by mechanical engineers and was closed in its own laboratory). Figure 1.3 shows some old Firenze Race Team cars, built from 2004 to 2007. A sort of tradition was always kept on by the team, that proposed very simple cars with strong components: the final aim of every project was to have really light and easy to build cars. Some of the most successful cars, like the F2005-V2 (that was probably the fastest car we ever made) have their strength in the extreme low mass and in the exceptional handling.

Figure 1.3 - Old Firenze Race Team cars: F2004-V2ss, F2005-V2 and F2007-V2

Many things changed during the last years of activity. The old name, Team V2, changed to Firenze Race Team and the team started to search people outside our department, pointing to be as similar as possible to the great European teams that were overbearingly coming out. The last car, the 2708RR, is, in a certain way, a complete new product for what concerns ideas, shape and competences used in it.

It can be said that the slow transformation of the team reflected in its last car, shown in Figure 1.4: Firenze Race Team expanded and now it includes students not only from mechanical engineering but also from electronic engineer, energy engineer, telecommunications engineer and other faculty like economy,

marketing and design. As a matter of facts the last year car and, hopefully, the future ones, have much more electronic devices, more studies on engine and aerodynamics and more studies on the marketing and cost analysis part.

Figure 1.4 - The 2708RR car

Many years passed from the birth of the Firenze Race Team and many really good students wrote their name in its history; after ten years the team is still here, facing new challenges with the same enthusiasm and giving the students the opportunity to prove themselves in the real world of competitions and designing.

2 Vehicle dynamics

2.1 Simple models

Before starting with the proper explanation of the vehicle model fitted with a locking differential a brief review of the basics vehicle models is presented.

The meaning of studying the directional behavior of a vehicle is, synthesizing, to find a correlation between the driver input and the path followed by the vehicle. Particularly we try to find out how, using the same inputs, the dynamic behavior of the vehicle is influenced by its constructive parameters, like geometry, inertial data, suspensions, tyres, etc.

The first temptation, when building a vehicle model, is to create a very complete one, effectively trying to insert all the parameters that rules over the body dynamic, in the hard effort to describe every single phenomena that interferes during vehicle motion. Unfortunately, very accurate models are, usually, very complicated both for formulation and results interpretation, so it's usually better to start a vehicle dynamics analysis with simple models, just to understand the main aspects of it without losing the main goal of the work.

In this chapter a brief review of two simple models is presented. For both the models some simplifications are introduced, particularly:

- The road is supposed to be straight and plain
- Pitch and shake are negligible due to the little advancement speed
- Roll is also negligible. To be more precise, we are going to neglect the *inertial actions due to roll* supposing to have really small chassis lateral inclinations, that imposes, as a matter of fact, to travel large radius turns. In case of a race car, having really stiff suspensions, roll chassis motions could be considered to be small even during small radius turns without introducing major errors.

- The vehicle is considered to be rigid, without any elastic element, like suspensions. Again this simplifications perfectly fits to race cars where suspensions are usually really stiff.
- Inertia of the wheels is neglected.
- Little steering angles are considered.

With all these simplifications and hypothesis these simples models only have three degrees of freedom where the vehicle is reduced to a single rigid body. It has to be noticed that, paradoxically, this models better fit to a race car than to a common car.

2.1.1 The bicycle vehicle model

The classical bicycle vehicle model is the most popular and largely used mathematical model for the analysis of the directional behavior of vehicles. Its properties have been largely described by many authors in their scientific papers [1], [2], [3], [4]. Even if largely studied we think to be convenient to briefly summarize this model again, to better understand the results of this thesis.

The bicycle vehicle model has been developed to reproduce the dynamic behavior of a rear-wheel drive vehicle fitted with an open differential: the vehicle model, as shown in Figure 2.1, is represented as a rigid body fitted with only two equivalent tyres, which have the duty to represent the front and the rear axles. The motion of the vehicle is, as said before, plane and parallel to the road. It's useful to define a reference frame (x, y, z, G) attached to the vehicle whose origin coincides with the center of mass *G* and whose versors are (**i**, **j**, **k**). Axes **i** and **j** are parallel to the road. The direction of axis **i** coincides with the forward direction of the vehicle while **j** is orthogonal to that direction. Axis **k** is orthogonal to the road and point upwards. Such a model has three state variables: the longitudinal speed *u*, the lateral speed *v* and the yaw rate *r*. The speeds *u* and *v* are the longitudinal and lateral components of the absolute speed $\mathbf{V_G}$ of the centre of mass *G*:

$$V_G = ui + vj \tag{2.1}$$

The yaw rate *r* is the only component of the angular velocity **Ω** of the vehicle: **Ω**=*r***k**. The slip angle β of the vehicle is defined as:

$$\beta = \arctan\left(\frac{v}{u}\right) \approx \frac{v}{u} \tag{2.2}$$

Still referring to Figure 2.1, a_1 and a_2 are the longitudinal distances between the centre of mass *G* and each axle, $l=a_1+a_2$ is the wheelbase, δ is the front steer angle, which is assumed to be small, i.e. δ≤15°.

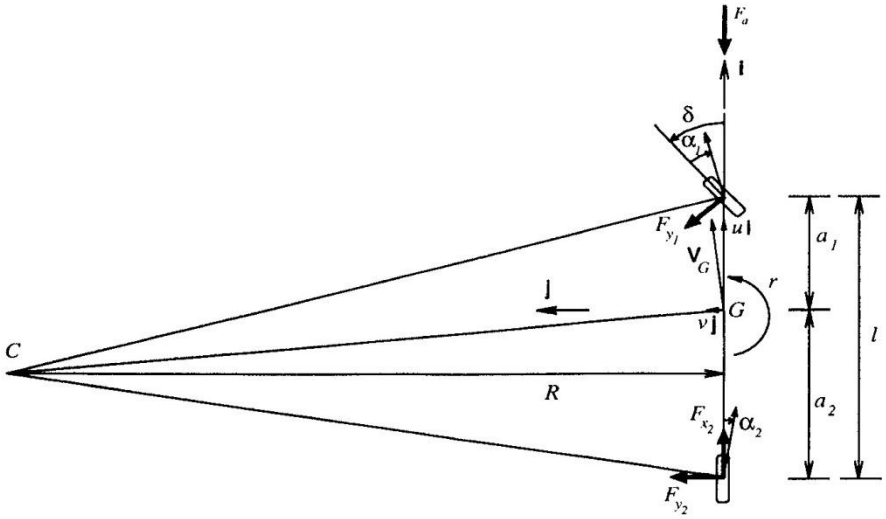

Figure 2.1 - The bicycle vehicle model

The front and rear slip angles are defined as:

$$\alpha_1 = \delta - \frac{v + ra_1}{u}$$
$$\alpha_2 = \delta - \frac{v - ra_2}{u} \tag{2.3}$$

The variable $R=u/r$ represents the distance between the instantaneous centre of rotation *C* of the vehicle and the longitudinal vehicle axis. In steady-state conditions (i.e., $\dot{u} = \dot{v} = \dot{r} = 0$) *R* is also the turning radius. The following important kinematic relation holds:

$$\delta - \frac{l}{R} = \alpha_1 - \alpha_2 \tag{2.4}$$

The quantity l/R is the so-called *Ackermann* steer angle. It represents the steer angle which is necessary to negotiate a corner with constant turning radius equal to *R*, when slip angles α_1 and α_2 are equal to zero.

The acceleration of the centre of mass *G* is:

$$a_G = \frac{dV_G}{d_t} = (\dot{u} - vr)i + (\dot{v} + ur)\,j = a_x i - a_y j \tag{2.5}$$

Where $a_x = (\dot{u} - vr)$ and $a_y = (\dot{v} + ur)$ are the longitudinal and lateral accelerations, respectively. In order to characterize the steady-state directional behavior of the vehicles, in which $\dot{u} = \dot{v} = \dot{r} = 0$, it is important to define the steady-state lateral acceleration:

$$\tilde{a}_y = ur = \frac{u^2}{R} \tag{2.6}$$

In Figure 2.1, forces F_{y1} and F_{y2} are the lateral forces acting on the front and rear equivalent tyres while F_{x2} is the longitudinal force. No longitudinal force acts on the front tyre as the rolling resistance is neglected and there is no motor torque on it (as we are considering a rear-wheel drive vehicle). The final equilibrium equations for the vehicle model are:

$$\begin{cases} m(\dot{u} - vr) = F_{x2} - F_{y1}\delta - F_a \\ m(\dot{v} + ur) = F_{y1} + F_{y2} \\ J_r = F_{y1}a_1 - F_{y2}a_2 \end{cases} \tag{2.7}$$

2.1.2 Revision of the handling diagram for the bicycle model

As we previously said, in the bicycle model, longitudinal slips are all neglected. Referring to [1], a non linear relationship between the whole lateral force and the slip angle of each axle can be found, written in the form:

$$\begin{aligned} F_{y1} &= F_{y1}(\alpha_1) \\ F_{y2} &= F_{y2}(\alpha_2) \end{aligned} \tag{2.8}$$

The relations (2.8) represent the cornering characteristics of the front and rear axles, respectively. It's now necessary to introduce two more constants,

respectively called W_1 and W_2, which are the vertical loads acting on the front and rear axles:

$$W_1 = \frac{mga_2}{l}$$
$$W_2 = \frac{mga_1}{l} \tag{2.9}$$

where we called *g* the acceleration of gravity. Under steady-state cornering conditions, starting from equation (2.7), it's possible to obtain the following relations:

$$\frac{F_{y1}(\alpha_1)}{W_1} = \frac{F_{y2}(\alpha_2)}{W_2} = \frac{\tilde{a}_y}{g} \tag{2.10}$$

Moreover, on the basis of equation (2.4) it's possible to obtain:

$$\frac{\tilde{a}_y}{g} = \frac{u^2}{gl}[\delta - (\alpha_1 - \alpha_2)] \tag{2.11}$$

Equations (2.10) and (2.11) define completely all the possible steady-state cornering conditions of the vehicle. Equation (2.10) represents a curve on a plane $(\tilde{a}_y/g\,, \alpha_1 - \alpha_2)$, which depends only on the constructive parameters of the vehicle (in Figure 2.2, it's the curve that passes from the origin). Equation (2.11) represents a straight line on the same plane, which is dependent from the parameters *u* and *δ* (it's, in Figure 2.2, the straight line on the left). Once the values of these parameters have been assigned, the intersection point between the line and the curve represents the corresponding equilibrium condition of the vehicle in the cornering manoeuvre defined by the actual values of *u* and δ (point *P* in Figure 2.2). The curve described by the equation (2.10) is the so called handling curve.

It has been demonstrated that, for a bicycle vehicle model, the difference between front and rear slip angles $(\alpha_1 - \alpha_2)$ depends only on the steady-state lateral acceleration $\tilde{a}_y$. At a given equilibrium condition *P*, it is possible to identify two particular slip angles α_1 and α_2.

Moreover the corresponding value of the ratio l/R_p can be obtained using the equation (2.4). In Figure 2.2, it is possible to use an auxiliary straight line, parallel to the line (2.11) and passing through the origin, and thus obtain the value of l/R_p on the rightwards axis.

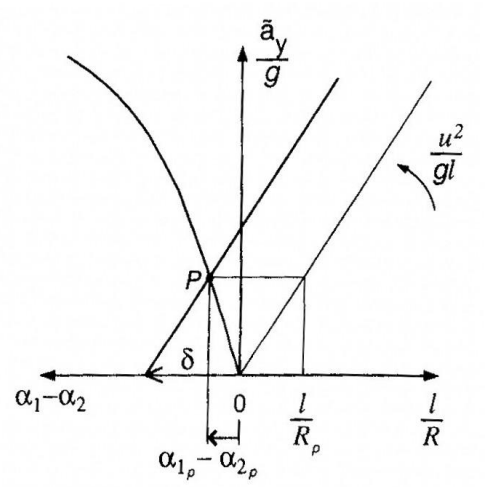

Figure 2.2 - Handling diagram for the bicycle model

According to [5] at each equilibrium condition we can define K as:

$$K = \frac{d}{d\tilde{a}_y}\left(\delta - \frac{l}{R}\right) = \frac{d}{d\tilde{a}_y}\left(\alpha_1 - \alpha_2\right) \tag{2.12}$$

K is commonly called *understeer gradient*, and it represents the slope of the handling curve at each equilibrium condition *P*.

The understeer-oversteer characteristics of the vehicle at each steady-state cornering condition *P* are defined as follows:

- *understeer* if $K > 0$;
- *neutral* if $K = 0$;
- *oversteer* if $K < 0$.

Let us introduce the cornering stiffness, defined as:

$$\Phi_1 = \left.\frac{dF_{y1}}{d\alpha_1}\right|_{\alpha_1=\alpha_{1P}} ; \quad \Phi_2 = \left.\frac{dF_{y2}}{d\alpha_2}\right|_{\alpha_2=\alpha_{2P}} \tag{2.13}$$

Which represent the slopes of the cornering characteristics of the front and rear axles, evaluated at the slip angles α_{1P} and α_{2P} which correspond to a given steady-state cornering condition *P*. The following relations can be obtained:

$$\frac{d\tilde{a}_y}{d\alpha_1} = \frac{\Phi_1 l}{a_2 m} \quad ; \quad \frac{d\tilde{a}_y}{d\alpha_2} = \frac{\Phi_2 l}{a_1 m} \tag{2.14}$$

Therefore, the understeer gradient *K* is given by:

$$K = \frac{m}{l}\left(\frac{\Phi_2 a_2 - \Phi_1 a_1}{\Phi_1 \Phi_2}\right) \tag{2.15}$$

Summing up, for the classical bicycle vehicle model the handling diagram depends only upon the constructive features of the vehicle. Accordingly, the understeer gradient depends only on the steady-state lateral acceleration $\tilde{a}_y$, and therefore on the steady-state cornering condition (point *P* in Figure 2.2). Therefore, the handling diagram and the understeer-oversteer characteristics do not depend on the particular manoeuvre performed. As it will be further demonstrated, these results are valid only for the very particular bicycle model since, in general, there is a strong dependence on the manoeuvre.

2.1.3 Model of vehicle with locked differential

Using the same simplifications introduced at the beginning of this chapter it's possible to develop a second model of car, having four wheels and a locked differential. The reference frame (x, y, z, G) is the same defined for the bicycle model, like the center of mass *G* and the versors are (**i**, **j**, **k**).

The vehicle model that has been considered in this paragraph will be used, once rebuilt in Simulink® environment, as a first model for the analysis of the differential influence on Formula SAE vehicles.

Generally, this reference frame is not coincident with the central inertial system but, if we assume the vehicle to be symmetrical respect to the longitudinal plane containing the axes *x* and *y*, than *y* is a central inertial axis so J_{xy} and J_{zy} are equal to zero.

The yaw rate *r* is the only component of the angular velocity **Ω** of the vehicle: **Ω**=*r***k**.

The absolute speed of the body is the same $\mathbf{V_G}$ described by equation (2.1). Referring to Figure 2.3, a_1 and a_2 are the distances of *G* from the front and

rear axles respectively; $l = a_1 + a_2$ is the wheelbase while t_1 and t_2 are the front and rear track of the vehicle. Considering the cinematic steering, that is the one with negligible slip angles, we have to precise that the steering angle δ_i of the internal wheel is bigger that the external one δ_e, according to the relation:

$$\frac{t_1}{l} = \frac{1}{\tan\delta_e} - \frac{1}{\tan\delta_i} \tag{2.16}$$

from which is possible to obtain [1]:

$$\delta_e = \delta_i - \frac{t_1}{l}\delta_i^2 + o\left(\begin{matrix}3\\ i\end{matrix}\right) \tag{2.17}$$

Therefore, having supposed small steering angles, we obtain $\delta_i \cong \delta_e$.

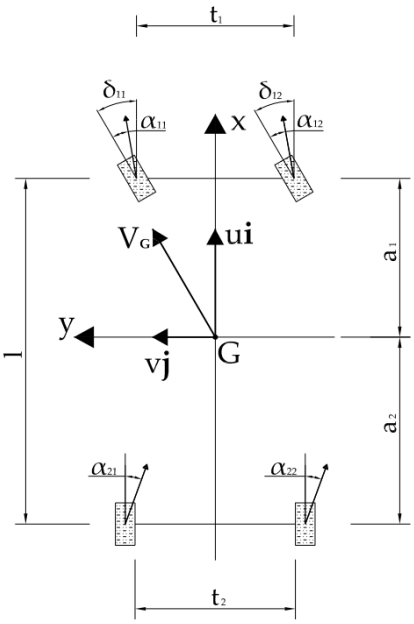

Figure 2.3 - Locked differential vehicle model

It's now possible to proceed to the formulation of the mathematical model, using three sets of equations: congruence equations, equilibrium equations and constitutive equations.

Congruence equations

The slip angle α defines the wheel center speed related to the longitudinal symmetry plane of the tyre. Considering the vehicle as a rigid body, the center of mass velocity $\boldsymbol{V_G}$ and the yaw speed *r* univocally define the four slip angles α_{ij} of the wheels. The *i* index defines the vehicle axle (*i*=1 for the front axle and *i*=2 for the rear one) and the *j* index defines the right or left tyre (*j*=1 for the left tyre and *j*=2 for the right one).

The same considerations of the bicycle model are still effective and the equations (2.1), (2.2), (2.3) and (2.10)(2.4) are still valid. Considering the absolute velocities of the wheel centers, and applying the rigid body kinematic fundamental formula it's possible to write:

$$\begin{cases} V_{11} = \left(u - \dfrac{rt_1}{2}\right) i + \left(v + ra_1\right) j \\ V_{12} = \left(u + \dfrac{rt_1}{2}\right) i + \left(v + ra_1\right) j \\ V_{21} = \left(u - \dfrac{rt_2}{2}\right) i + \left(v - ra_2\right) j \\ V_{22} = \left(u + \dfrac{rt_2}{2}\right) i + \left(v - ra_2\right) j \end{cases} \tag{2.18}$$

It's immediate to write the following equations:

$$\begin{cases} \tan\left(\delta - \alpha_{11}\right) = \dfrac{v + ra_1}{u - r\dfrac{t_1}{2}} \\ \tan\left(\delta - \alpha_{12}\right) = \dfrac{v + ra_1}{u + r\dfrac{t_1}{2}} \\ \tan\left(-\alpha_{21}\right) = \dfrac{v - ra_2}{u - r\dfrac{t_2}{2}} \\ \tan\left(-\alpha_{22}\right) = \dfrac{v - ra_2}{u + r\dfrac{t_2}{2}} \end{cases} \tag{2.19}$$

Considering that, in normal condition, $u \gg \frac{|r|t_1}{2}$, it's possible to notice that the two slip angles of the wheels from the same axle are almost the same; it's

so possible to refer with α_1 to the front slip angles and with α_2 to the rear one. The previous equations become:

$$\begin{cases} \tan(\delta - \alpha_1) = \dfrac{v + ra_1}{u} \\ \tan(-\alpha_2) = \dfrac{v - ra_2}{u} \end{cases} \tag{2.20}$$

It's possible to further simplify these expressions, considering that $u \gg v$ and $u \gg |r|a_1$ and, consequently, in equations (2.2) and(2.3) (2.20) considering that $arctan \cong tan$ and obtaining the linearized form:

$$\begin{cases} (\delta - \alpha_1) = \dfrac{v + ra_1}{u} \\ (-\alpha_2) = \dfrac{v - ra_2}{u} \\ \beta = \dfrac{v}{u} \end{cases} \tag{2.21}$$

That relate the velocities *u*, *v* and *r* to the slip angles α_1 and α_2.

Equilibrium equations

It's possible to express the equilibrium equations using the dynamic cardinal equations, thus obtaining:

$$ma_g = F \tag{2.22}$$

$$J_z\dot{\Omega} = M_G \tag{2.23}$$

It has to be noticed that, writing the equation (2.23), the term J_{xy} has been neglected due to the fact that this is usually really small compared to J_z.

Referring to the system $(x, y, z; G)$, we have:

$$a_G = a_x i + a_y j \tag{2.24}$$

$$\dot{\Omega} = \dot{r}k \tag{2.25}$$

And

$$F = Xi + Yj + Zk \tag{2.26}$$

$$M_G = Nk \tag{2.27}$$

It's so necessary to calculate the accelerations of G and the force acting on the whole system. For shortness of treatment the calculation of these accelerations and forces is omitted and only the results are reported.

Accelerations

The considered accelerations are:

- **Acceleration of the center of mass:**

$$\begin{aligned} a_G &= \frac{dV_G}{dt} = \dot{u}i + urj + \dot{v}j - vrj = \\ &= (\dot{u} - vr)i + (\dot{v} + ur)j = \\ &= a_x i + a_y j \end{aligned} \tag{2.28}$$

thus obtaining:

$$a_x = \dot{u} - vr \tag{2.29}$$

$$a_y = \dot{v} + ur = \dot{v} + \frac{u^2}{R} \tag{2.30}$$

That are the longitudinal and lateral accelerations.

- **Stationary lateral acceleration**

$$\tilde{a}_y = ur = \frac{u^2}{R} \tag{2.31}$$

so, using this expression, it's possible to write the (2.30) as:

$$a_y = \dot{v} + \tilde{a}_y \tag{2.32}$$

- **Angular acceleration**

Simply obtained deriving *r*:

$$\dot{\Omega} = (0,0,\dot{r}) \tag{2.33}$$

Forces and momentums

The forces and momentums acting on the vehicle are: the weight force due to gravity, the reactions acting on the wheels due to the road-tyre contact and the aerodynamic force due to the presence of air.

The three equilibrium equations (in the Newtonian form) necessary to describe the motion of a rigid body in space are:

$$\begin{cases} ma_x = X \\ ma_y = Y \\ J\dot{r} = N \end{cases} \tag{2.34}$$

Where $X = \sum longitudinal\ forces$, $Y = \sum lateral\ forces$ and $N = \sum yaw\ momentums$. For what concerns the weight force acting on the vehicle it has to be valid at every instant (as considering a planar motion) the relation:

$$ma_z = Z = 0 \tag{2.35}$$

Where $Z = \sum vertical\ forces = 0$.

Referring to Figure 2.4, we call $F_{x_{ij}}$ the longitudinal components of the tangential forces acting between the four tyres and the road, and with $F_{y_{ij}}$ the lateral components of the same forces. All the auto-aligning moments $M_{z_{ij}}$ have been neglected due to their little influence on the vehicle dynamic [1].

The other force that has to be considered is the aerodynamic force acting on the vehicle. In this treatment only the aerodynamic resistance F_{ax} has been considered. Aerodynamic force can so be written as:

$$F_a = F_{ax} i = -\frac{1}{2}\rho S C_x u^2 i \tag{2.36}$$

Where:

- ρ = air density
- S = frontal surface of the vehicle
- C_x = aerodynamic resistance coefficient.

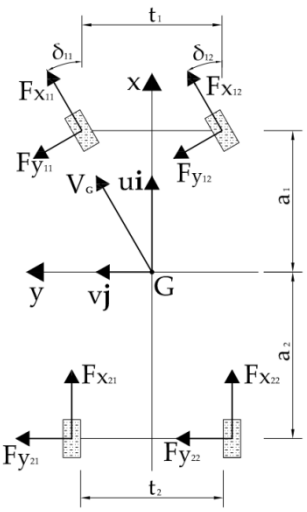

Figure 2.4 - Forces acting on wheels

Considering that for steering angle smaller than 15° (≅ 0,26rad) it's possible to put $\cos\delta = 1$ and $\sin\delta = \delta$ and considering the forces acting on the vehicle, it's possible to write:

$$m(\dot{u} - vr) = \left(F_{x_{11}} + F_{x_{12}}\right) + \left(F_{x_{21}} + F_{x_{22}}\right) - \left(F_{y_{11}} + F_{y_{12}}\right)\delta_1 - F_{ax} \tag{2.37}$$

$$m(\dot{v} + ur) = \left(F_{x_{11}} + F_{x_{12}}\right)\delta_1 + \left(F_{y_{11}} + F_{y_{12}}\right) + \left(F_{y_{21}} + F_{y_{22}}\right) \tag{2.38}$$

$$\begin{aligned} J\dot{r} &= \left[\left(F_{x_{11}} + F_{x_{12}}\right)\delta_1 + \left(F_{y_{11}} + F_{y_{12}}\right)\right]a_1 - \left(F_{y_{21}} + F_{y_{22}}\right)a_2 + \\ &= -\left(F_{x_{11}} - F_{x_{12}}\right)\frac{t_1}{2} - \left(F_{x_{21}} - F_{x_{22}}\right)\frac{t_2}{2} + \left(F_{y_{11}} - F_{y_{12}}\right)\delta_1\frac{t_1}{2} \end{aligned} \tag{2.39}$$

To simplify the previous equations it's possible to sum together the forces acting on a same axle:

$$\begin{cases} F_{x_1} = F_{x_{11}} + F_{x_{12}} \\ F_{x_2} = F_{x_{21}} + F_{x_{22}} \\ F_{y_1} = F_{y_{11}} + F_{y_{12}} \\ F_{y_2} = F_{y_{21}} + F_{y_{22}} \end{cases} \tag{2.40}$$

Considering only two wheel drive vehicles with only front steering and rear traction it's possible to neglect the rolling resistance of the front tyre, thus writing:

$$F_{x_{11}} = F_{x_{12}} = 0$$

Considering that the rear wheels don't have the steering degree of freedom, it's possible to write $\left(F_{y_{21}} - F_{y_{22}}\right)\delta_2 t_2/2 = 0$. Concerning to what we said, it's possible to write:

$$\begin{cases} m\left(\dot{u} - vr\right) = F_{x_2} + F_{y_1}\delta_1 - F_{ax} \\ m\left(\dot{v} + ur\right) = F_{y_1} + F_{y_2} \\ J\dot{r} = F_{y_1}a_1 - F_{y_2}a_2 + \left(F_{y_{11}} - F_{y_{12}}\right)\delta_1 \dfrac{t_1}{2} + M_{z_2} \end{cases} \tag{2.41}$$

Vertical load on tyres

Load variations on each tyre depends on the load transfers, both longitudinal and lateral. In this case roll and pitch motions are neglected, so as the presence of suspensions; load transfers are instantaneous.

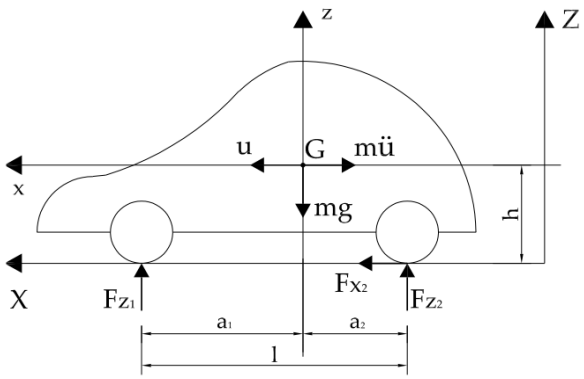

Figure 2.5 - Longitudinal load transfer

Longitudinal load transfer due to longitudinal acceleration is, referring to Figure 2.5:

$$\begin{cases} F_{x_2} = m\dot{u} \\ F_{z_1} + F_{z_2} = mg \\ F_{z_2} a_2 - F_{z_1} a_1 - F_{x_2} h = 0 \end{cases} \tag{2.42}$$

whence is possible to obtain:

$$\begin{cases} F_{z_1} = \dfrac{mga_2}{l} - \dfrac{mh}{l}\dot{u} \\ F_{z_2} = \dfrac{mga_1}{l} + \dfrac{mh}{l}\dot{u} \end{cases} \tag{2.43}$$

where $\frac{mg\,a_2}{l}$ is called *static load* of the front axle and is usually shown as F_{z1}^0; the same for the rear axle: $F_{z2}^0 = \frac{mg\,a_1}{l}$. Applying these equations it's possible to obtain:

$$\begin{cases} \Delta F_{z_{11}}^{x} = \Delta F_{z_{12}}^{x} = -\dfrac{mh}{2l}\dot{u} \\ \Delta F_{z_{21}}^{x} = \Delta F_{z_{22}}^{x} = \dfrac{mh}{2l}\dot{u} \end{cases} \tag{2.44}$$

Where *h* is the height of the center of mass *G* and *l* is the wheelbase. The derivative $\dot{u}$ is positive during acceleration and negative during deceleration.

Considering Figure 2.6, and using the simplifications described at the beginning of this chapter, it possible to simply calculate the lateral load transfers due to the lateral acceleration a_y acting on *G*, performing a static load balance [1]:

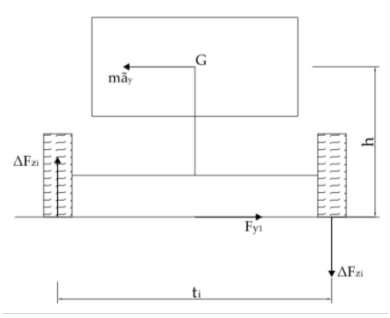

Figure 2.6 - Lateral load transfer

$$\begin{cases} F_{y_1} + F_{y_2} = ma_y \\ F_{y_1} a_1 - F_{y_2} a_2 = J\dot{r} \\ \Delta F_{z_1}^{y} + F_{y_1} h = 0 \\ \Delta F_{z_2}^{y} + F_{y_2} h = 0 \end{cases} \tag{2.45}$$

whence is possible to determine the load transfers due to transversal accelerations:

$$\begin{aligned} \Delta F_{z_{11}}^{y} &= \Delta F_{z_{12}}^{y} = mB_1 a_y \\ \Delta F_{z_{12}}^{y} &= \Delta F_{z_{22}}^{y} = mB_2 a_y \end{aligned} \tag{2.46}$$

where the constants B_1 and B_2 are equal to:

$$B_1 = \frac{1}{t_1}\left(\frac{ha_2}{l}\right); B_2 = \frac{1}{t_2}\left(\frac{ha_1}{l}\right)$$

Once the static loads are known, and adding to them the lateral and longitudinal load transfers, it's possible to obtain the vertical loads acting on tyres, that are:

$$\begin{cases} F_{z_{11}} = F_{z_{11}}^{0} - mB_1 a_y - \dfrac{mh}{2l}\dot{u} \\ F_{z_{12}} = F_{z_{12}}^{0} + mB_1 a_y - \dfrac{mh}{2l}\dot{u} \\ F_{z_{21}} = F_{z_{21}}^{0} - mB_2 a_y + \dfrac{mh}{2l}\dot{u} \\ F_{z_{22}} = F_{z_{22}}^{0} + mB_2 a_y + \dfrac{mh}{2l}\dot{u} \end{cases} \tag{2.47}$$

Constitutive equations

The vehicle model could be considered complete only when the behavior of each tyre has been defined, in terms of relations between the tangential forces (that the road applies on tyre) and slip angles, vertical load, camber angle and

longitudinal slip. Many formulations of these relations can be applied, considering different behavior for the tyres: one approach considers a linear tyre model with an immediate response of it to stresses, while others suppose that the tyre response is retarded, modeling the relaxing length with a differential equation [1].

Deciding to renounce to the hypothesis of response linearity it's possible to improve the model complexity and accuracy by the use of empiric formulae, like the *Magic Formula* [6]. Due to the fact that we are going to develop some vehicle models closely related to reality and to calibrate it on a real existing Formula SAE car (the 2708RR of the Firenze Race Team), it has been decided to follow a non linear, empiric formulation for tyres behavior, thus using the Pacejka *Magic Formula*. The common expression of this formula is:

$$y(\chi) = D\sin\left(C\tan^{-1}\left(B\chi - E\left[B\chi - \tan^{-1}(B\chi)\right]\right)\right) \qquad (2.48)$$

where χ is the free variable and could gain the meaning of slip angle α if y has is the lateral force F_y, or longitudinal slip s_x if y is the longitudinal force F_x. The four parameters B, C, D and E are determined in order to obtain the behavior of the experimental curves.

2.1.4 Motion transmission

As the vehicle model with locked differential will also be used as a comparison in the next chapter, it's interesting to spend some words on the motion transmission, in order to understand how it'll be modeled afterwards. Due to the fact that we are interested in the differential influence on vehicle dynamics, the entire driveline will be schematized in a simple way, avoiding a particular treatment. Figure 2.7 shows the driveline scheme, where:

- Ω_{m} is the angular velocity of the crankshaft
- Ω_{p} is the primary gear shaft angular velocity
- Ω_{s} is the secondary gear shaft angular velocity
- Ω_{dif} is the differential box angular velocity

It has to be noticed that if the clutch is engaged we have $\Omega_{\mathrm{m}} = \Omega_{\mathrm{p}}$.

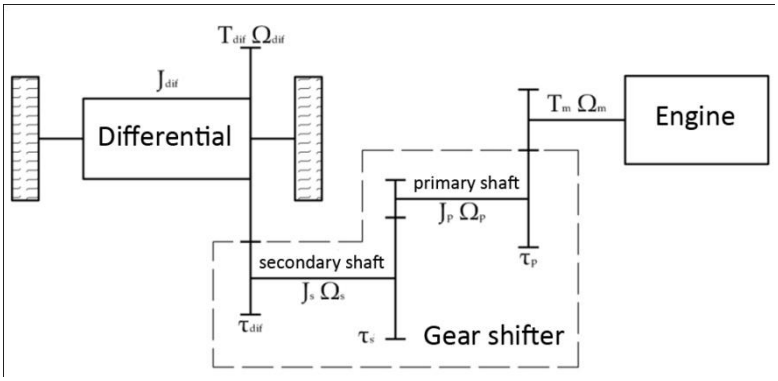

Figure 2.7 - Driveline scheme

To calculate the torque acting on the differential box, the following transmission ratios have been used:

$$\tau_p = \frac{\Omega_m}{\Omega_p}$$
$$\tau_s = \frac{\Omega_p}{\Omega_s} \tag{2.49}$$
$$\tau_{diff} = \frac{\Omega_s}{\Omega_{diff}}$$

The transmission ration τ_s depends on the gear in use and τ_{diff} is the final transmission ratio that, considering the 2708RR (the last car built by the Firenze Race Team), is the ratio between the front and rear sprocket teeth. It's now possible to define a total transmission ratio as:

$$\tau_t = \tau_p \tau_s \tau_{diff} \tag{2.50}$$

It's proper to remember that the inertial momentums J_m, J_p, J_s and J_{diff} are related to the rotating masses at the speed of the crankshaft, the primary shaft, the secondary shaft and the differential carter.

Considering the clutch to be engaged, it's possible to apply to the powertrain group the energy conservation theorem. The input power in the system is the engine one, given by the product between the torque T_m and the revolution speed Ω_{m}. The output power is given by the product of the torque acting on the

differential T_{diff} and the angular velocity of the differential housing Ω_{diff}. If we name with η_t the gearshift efficiency, it's possible to write:

$$\eta_t \mathrm{P}_m - T_{diff}\Omega_{diff} = \frac{dE_c}{dt} \tag{2.51}$$

The gear shifter group kinetic energy is:

$$E_c = \frac{1}{2}J_m\Omega_m^2 + \frac{1}{2}J_p\Omega_p^2 + \frac{1}{2}J_s\Omega_s^2 \tag{2.52}$$

From the two expression above it's possible to obtain the expression of the torque acting from the gear shifter to the differential housing:

$$T_{diff} = \eta_t\tau_t T_m - J_m\tau_t\dot{\Omega}_m - J_p\tau_s\tau_{diff}\dot{\Omega}_p - J_s\tau_{diff}\dot{\Omega}_s \tag{2.53}$$

It's interesting to notice that the inertial rates due to the clutch and to the selected gear are effectively taken into account inside the model. Otherwise the torsional contributions have been neglected as no structural calculations will be done. Figure 2.8 illustrates the differential scheme. The reference system used $(x_o, y_o, z_o; O)$ is united to the differential housing.

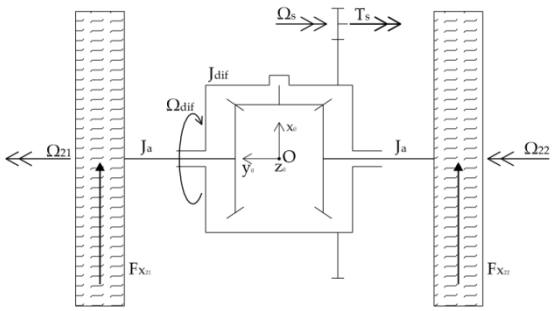

Figure 2.8 - Differential and wheels scheme

Origin O, coincides with the center of the differential housing, the axis x_o coincides with the pinion gear axis and the axis y_0 is parallel to the axis y, that is united to the vehicle. The proposed driveline scheme, as the whole rigid vehicle model, will be afterwards used when the self-locking differential will be modeled.

2.1.5 Rear wheels equilibrium equation

In this model a completely locked differential is considered, so the two half shafts have, in every moment, the same angular velocity ($\varpi_{21} = \varpi_{22} = \Omega_2$). It's so permitted to consider the half shafts as being only one, and so writing the equilibrium equation for the entire axle:

$$T_{diff} - F_{x2} R_{sc2} = 2 J_a \dot{\Omega}_2 \tag{2.54}$$

where R_{sc2} is the rear wheel radius under load conditions (usually considered the same as R) and T_{diff} is the engine torque reduced to the axle and is a driving parameter, directly controlled by the driver.

3 3 DOF vehicle model

3.1 Analyzed vehicles: differential models

Starting from the rigid vehicle model with locked differential, it has been logic to follow a model evolution, implementing the limited slip differential that, actually, the Firenze Race Team uses on its cars. In this chapter the characteristics of different typologies of transmissions will be analyzed, from the locked differential to the self locking one. For the last one, the limited slip differential (LSD), all the equations used to characterize it will be presented; it will also be used as a base for the Matlab/Simulink® model implementation built to characterize both the longitudinal and lateral dynamic behavior of the 2708RR car.

Just to introduce the treatment of this paragraph let's remind that the differential is a mechanic device that has the duty to transfer the engine torque to the wheels, dividing it properly, independently from the angular velocity of the wheels. It's so obvious to understand that the duty of the differential is crucial to grant the correct contact between road and tyre during cornering.

As it will be afterwards shown, the differential influence is also very important for what concern the lateral and longitudinal behavior of the car. The way it divides the torque between the two half shafts has a great influence over the under/oversteer behavior of the car, with great repercussions on vehicle stability.

3.1.1 Rigid axle

The easiest way to connect two drive wheels is by the use of a rigid axle, effectively connecting the two tyres. A mathematical treatment of this kind of transmission has been explained in section 2.1.3. This solution, has been adopted on the first models of vehicles and is, indeed, easy to build and particularly cheap; that's why it's commonly used on karts. The rigid axle solution is particularly useful when the two wheels of an axle are working with different adherence conditions, like on off-road vehicles (usually fit with a lockable differential, thus acting as a rigid

axle), but it cannot satisfy the kinematic cornering conditions, thus leading the vehicle to a great instability (effectively loosing directional capabilities).

3.1.2 Open differential

The open differential allows two wheels of the same axle to rotate, during cornering, with different speeds, thus satisfying the kinematic conditions. As shown in Figure 3.1, the open differential is an epicyclical gearing that transmits the torque from the housing (or cage) to the axles through the side gears.

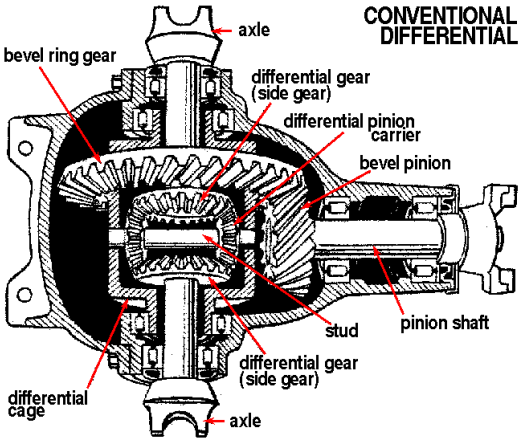

Figure 3.1- Section of an open differential

The differential housing, or cage, is joint to the bevel ring gear and rotates at an angular speed Ω_{diff}, receiving from the gearbox the torque T_{diff}. This torque is redirected to the side gears, so to the half shafts, that rotate with the angular velocities ω_1 and ω_2. The Willis formula, applied to a differential with the same teeth number for the two side gears ($z_1 = z_2$), gives us the relation between the bevel ring gear and the side gears speeds:

$$\tau_0 = \frac{\omega_{22} - \Omega_{diff}}{\omega_{21} - \Omega_{diff}} = -1 \tag{3.55}$$

from which is possible to obtain:

$$\Omega_{diff} = \frac{\omega_{21} + \omega_{22}}{2} \tag{3.56}$$

It's now possible to obtain the expressions that link the torques of the two drive shafts, T_1 and T_2, to the one coming from the differential T_{diff} :

$$\begin{cases} T_{diff} - T_{21} - T_{22} = 0 \\ T_{diff}\Omega_{diff} - T_{21}\omega_{21} - T_{22}\omega_{22} - W_{lost} = 0 \\ \Omega_{diff} = \dfrac{\omega_{21} + \omega_{22}}{2} \end{cases} \tag{3.57}$$

where W_{lost} is the power lost due to internal frictions that can be written as:

$$W_{lost} = C_f \left| \omega_{21} - \omega_{22} \right| \tag{3.58}$$

where C_f is the internal friction torque.

Resolving the balance of the (3.57) it's possible to obtain the expressions for the torque:

$$\begin{cases} T_{21} = \dfrac{T_{diff}}{2} - C_f \dfrac{\left| \omega_{21} - \omega_{22} \right|}{\omega_{21} - \omega_{22}} \\ T_{22} = \dfrac{T_{diff}}{2} + C_f \dfrac{\left| \omega_{21} - \omega_{22} \right|}{\omega_{21} - \omega_{22}} \end{cases} \tag{3.59}$$

In case that $\omega_1 \neq \omega_2$ the transmitted torques are:

$$\bullet\ \omega_{21} > \omega_{22} : \begin{cases} T_{21} = \dfrac{T_{diff}}{2} - C_f \\ T_{22} = \dfrac{T_{diff}}{2} + C_f \end{cases} \tag{3.60}$$

$$\bullet\ \omega_{21} < \omega_{22} : \begin{cases} T_{21} = \dfrac{T_{diff}}{2} + C_f \\ T_{22} = \dfrac{T_{diff}}{2} - C_f \end{cases} \tag{3.61}$$

In case $\omega_1 = \omega_2$the equations (3.59) are impossible to be directly solved, as they contain the undetermined form $\frac{0}{0}$, so it's necessary to estimate the limit of the function having ω_1 tending to ω_2. In this case we obtain:

$$\begin{aligned} T_{21} &= \frac{T_{diff}}{2} \pm C_f \\ T_{22} &= \frac{T_{diff}}{2} \mp C_f \end{aligned} \tag{3.62}$$

The equations (3.60) and (3.61) show that the differential always transmits a greater torque to the shaft rotating at lower speed, due to internal frictions. It's possible to write:

$$C_f = \frac{|T_{21} - T_{22}|}{2} \tag{3.63}$$

Usually we have that $C_f = (0{,}05 \div 0{,}09)|T_{diff}|$. It's also possible to introduce the differential internal efficiency, η_0, that takes into account all the causes responsible of the difference of torque on the two wheels of an open differential:

$$\frac{T_{21}}{T_{22}} = \frac{1 - f \tan\vartheta}{1 + f \tan\vartheta} = \eta_0 \tag{3.64}$$

Where f is the friction coefficient and ϑ is the pressure angle. Rewriting the equations previously introduced for the differential we finally obtain:

$$C_f = \frac{T_{diff}}{2}\left(\frac{1-\eta_0}{1+\eta_0}\right) \tag{3.65}$$

It's now possible to define the *blocking ratio b* of the differential as the ratio between the torque difference of the two wheels and the torque T_{diff} acting on the differential housing:

$$b = \frac{|T_{22} - T_{21}|}{T_{diff}} = \frac{T_{22} - T_{21}}{T_{21} + T_{22}} = \frac{1-\eta_0}{1+\eta_0} \tag{3.66}$$

The blocking ratio *b* gives an indication on the torque difference that is possible to transmit to the wheels. An open differential transmits the torque symmetrically to the two wheels; this could be, in some situations, a bad thing, actually limiting the traction capability of the vehicle. In case a wheel looses all its adherence it increases its angular velocity while, as the differential housing speed is still the same, applying Willis formula, the other wheel decreases it. If this condition persists it could be possible to have the complete stop of the wheel in adherence with a sudden break of the tractive force; it's clear that the traction of the vehicle depends only from the wheel with the worst adherence conditions.

3.1.3 Self locking differential

The traction capability of a vehicle can be highly increased reducing the efficiency of the differential η_0, thus increasing the value of the friction torque C_f. Effectively, the raise of C_f, produces the increase of the difference of torque that the differential transmits to the wheels. This effect permits, in case of two wheels with different adherence, to increase the torque transmitted to the wheel with a greater adherence, thus granting traction to the vehicle. The idea of using an high C_f to increase the traction of a vehicle led to the development of the self locking differential.

Between all the different types of self locking differential we considered the limited slip differential (LSD), as this is the one that equips the Firenze Race Team car. In this particular differential the increase of C_f is demanded to some friction discs, alternatively joined to the differential housing and to the side gears.

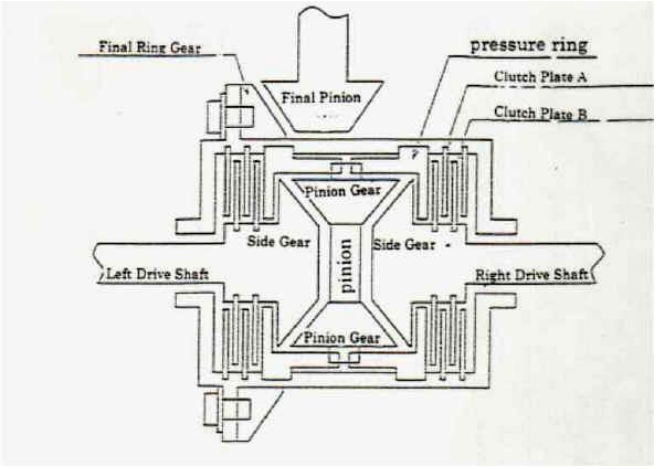

Figure 3.2 - Limited slip differential

As shown in Figure 3.2, the discs (clutch plates), are free to move axially and, in case of torque difference between the two axles, they are pushed together by the pressure ring. The braking torque acting between the differential housing and the side gears is:

$$M_b = k_{diff} \frac{T_{diff}}{2} \tag{3.67}$$

where k_{diff} is a constant depending from some building parameters of the clutches and from the inclination angle of the pushing rings surfaces, α.

Applying the superposition principle to the half shafts is possible to add the contribution of the clutches to the torque, thus having:

$$\begin{cases} T_{21} = \frac{T_{diff}}{2}\left(1 - \frac{1-\eta_0}{1+\eta_0}\right) - M_b = \frac{T_{diff}}{2}\left(1 - \frac{1-\eta_0}{1+\eta_0} - k_{diff}\right) \\ T_{22} = \frac{T_{diff}}{2}\left(1 + \frac{1-\eta_0}{1+\eta_0}\right) + M_b = \frac{T_{diff}}{2}\left(1 + \frac{1-\eta_0}{1+\eta_0} + k_{diff}\right) \end{cases} \tag{3.68}$$

The difference between the two motor torques ΔT, called *torque displacement*, is so:

$$\Delta T = |T_{22} - T_{21}| = T_{diff}\left(\frac{1-\eta_0}{1+\eta_0}\right) + k_{diff} \tag{3.69}$$

And the locking ratio is:

$$b = \frac{|T_{22} - T_{21}|}{T_{diff}} = \frac{1-\eta_0}{1+\eta_0} + k_{diff} \tag{3.70}$$

It has to be noticed that the LSD is almost the same as an open differential, with the only exception of the internal efficiency. For this kind of differential the locking ratio is constant, as the LSD is torque sensitive. The motor torque percentage distribution is independent from T_{diff}, and is constant in every condition, just like in an open differential.

3.2 LSD vehicle model

For this model, the same considerations on the rigid axle model are considered. The same congruence, equilibrium and constitutive equations are assumed to be valid. The great difference between the two models is that, having a LSD, the rear wheels cannot be considered rigidly connected: as a matter of fact two equations are requested for the rear wheels equilibrium, one for each wheel:

$$\begin{cases} T_{21} = \dfrac{T_{diff}}{2}\left(1 - \dfrac{1-\eta_0}{1+\eta_0}\operatorname{sgn}(\Delta\omega) - k_{diff}\operatorname{sgn}(\Delta\omega)\right) \\ T_{22} = \dfrac{T_{diff}}{2}\left(1 + \dfrac{1-\eta_0}{1+\eta_0}\operatorname{sgn}(\Delta\omega) + k_{diff}\operatorname{sgn}(\Delta\omega)\right) \end{cases} \tag{3.71}$$

where $\Delta\omega = \omega_{21} - \omega_{22}$ is the difference between the two angular velocities. Imposing the rotation equilibrium of the half shaft – wheel group, we have:

$$T_{2j} - F_{x_{2j}} R_{2j} = J_{a_{2j}} \dot{\omega}_{2j} \tag{3.72}$$

With $j = 1,2$ and where $F_{x_{2j}}$ is the longitudinal force acting between tyre and road, R_{2j} is the wheel radius and J_{2j} is the wheel and half shaft inertia. Substituting the (3.71) in the (3.72) we obtain:

$$\frac{T_{diff}}{2}\left(1 \pm \frac{1-\eta_0}{1+\eta_0}\operatorname{sgn}(\Delta\omega) \pm k_{diff}\operatorname{sgn}(\Delta\omega)\right) - F_{x_{2j}} R_{2j} = J_{a_{2j}} \dot{\Omega}_{2j} \tag{3.73}$$

This relation cannot be used if $\omega_{21} = \omega_{22} = \Omega_2$. Summing up, the equations that are used to write the LSD vehicle model are:

- Three vehicle equilibrium equations:

$$\begin{cases} m(\dot{u} - vr) = F_{x_2} + F_{y_1}\delta_1 - F_a \\ m(\dot{v} + ur) = F_{y_1} + F_{y_2} \\ J\dot{r} = F_{y_1}a_1 - F_{y_2}a_2 + (F_{y_{11}} - F_{y_{12}})\delta_1 \frac{t_1}{2} + M_{z_2} \end{cases} \tag{3.74}$$

- Two equilibrium equations for the rear tyres:

$$\begin{cases} T_{21} - F_{x_{21}}R_{21} = J_{a_{21}}\dot{\Omega}_{21} \\ T_{22} - F_{x_{22}}R_{22} = J_{a_{22}}\dot{\Omega}_{22} \end{cases} \tag{3.75}$$

- Eight constitutive equations:

$$\begin{cases} F_x = -\frac{\sigma_x}{\sigma} F_t(\sigma, \pm\Delta F_{z_{ij}}) \\ F_y = -\frac{\sigma_y}{\sigma} F_t(\sigma, \pm\Delta F_{z_{ij}}) \end{cases} \tag{3.76}$$

There have also to be considered eight other congruence equations that define the slip vectors and the vertical load on each tyre. The unknowns are the longitudinal speed u, the lateral speed v, the yaw speed r, the rear wheels speed Ω_{21}, Ω_{22}, the four lateral forces on tyres $F_{y_{ij}}$, the two longitudinal forces $F_{x_{ij}}$ and the four vertical loads $F_{z_{ij}}$. Two more parameters are needed to define the maneuvers: the engine torque T_m and the steering angle δ. We have a total of 17 equations and 17 unknowns.

3.3 Simulink® model implementation

In order to evaluate the behavior of the Firenze Race Team car on track, the equations previously described have been written in a Simulink® model, obtaining a simple and quite fast tool. Every single equation or system of equations have been rewritten and schematized with a block, making them explicit.

3.3.1 Motion equations

The three motion equations (considering a planar motion) have been made explicit as a function of the three accelerations: longitudinal, lateral and yaw around z axis. For each degree of freedom (DOF) a single block have been realized where the steering angle, the longitudinal forces, the lateral forces and the momentums around z are the inputs and the three accelerations (from which is possible to obtain the velocities) are the outputs. These three blocks have been composed to form a *vehicle dynamics* block from which is possible to deduce the accelerations and speeds of the center of mass, so the yaw speed and acceleration.

3.3.2 Congruence equations

As it was previously said the slip angles of the tyres on the same axle have been considered to be equals. In this way only two congruence equations are requested: one for the front axle slip angle calculation, and one for the rear. The equations have been made explicit as functions of the two slip angles and have been written as two blocks, one for each axle. The inputs values are the three velocities and, for the front axle, the steering angle; the outputs are the slip angles.

3.3.3 Vertical equilibrium on tyres

Four subsystems have been created in order to compute the vertical loads on tyres, starting from the static loads and the accelerations (both longitudinal and lateral) of the vehicle. A single subsystem calculating these loads have been created for each tyre.

3.3.4 Tyres slips

Tyres slips are calculated by a subsystem containing two blocks. In this first phase only the rear tyres have been considered, as the braking phase is not

taken into account. Further on the model have been modified to include the braking capability, so a new block has been added to the model to take into account the longitudinal forces on front tyres.

Each single subsystem calculates the slip of the tyre, having as inputs the rotational speed, the longitudinal and the yaw speed of the vehicle.

3.3.5 Constitutive equations

To integrate the constitutive equations of the tyre, the *Magic Formula* of Pacejka has been used. There are two subsystems for each tyre that have, as inputs, the camber and slip angles, the tyres slips and the vertical loads on each tyre. As outputs it's possible to obtain the longitudinal and lateral forces on each tyre.

3.3.6 Model inputs

Due to the model structure, the inputs needed to run the simulations are the parameters on which the driver has a control, that are:

- The steering angle
- The engine RPM
- The throttle body valve opening
- The selected gear

With the only exception of the gear, that is inserted in the model as a constant, all the other parameters could be controlled as a signal variable with simulation time. It's so possible to reproduce the experimental testes done on the real car on track and to confront the obtained results.

it's interesting to note that the engine has been characterized for its whole range of operation, using the data provided by a thermodynamic model developed inside the Firenze Race Team. This model reproduce the behavior of the Desmo3 Ducati engine as a function of the RPM and the load (in terms of throttle valve opening percentage. The considered loads are 10, 25, 50, 75 and 100%). These data have been inserted in the model as *2D Lookup table* that interpolates, using the engine data from the thermodynamic model, the throttle valve inputs with the RPM inputs and gives back as output the engine torque.

Another note is necessary for what concern the LSD, especially for its transition between the locked and unlocked condition. To have a differential able to fit the different working condition, it was necessary to develop a control logic that has to be simple and capable to define the correct transmitted torque to the

axis. To proper represent this transition, the first idea was to use the internal differential components friction coefficients and introduce them in the block, but this could result in a complication. It was also impossible to find all the needed friction coefficients, so this way was abandoned. Another idea could be to use a simple switcher, able to apply the different equations for both straight and turning condition: a simple check on the steering angle tells the system in what working condition the model is and chooses between the equations for $\omega_1 = \omega_2$ or $\omega_1 \neq \omega_2$. Again, this simple switcher introduces some hard discontinuities and is not suitable to model a continuous vehicle motion.

In the end it was decided to adopt a single state control logic, able to model the whole LSD behavior for every motion condition. This block introduces the equations (3.71) in the Simulink® model using the form:

$$\begin{cases} T_1 = \dfrac{T_{diff}}{2}\left(1 - p\dfrac{1-\eta_0}{1+\eta_0} - pk_{diff}\right) \\ T_2 = \dfrac{T_{diff}}{2}\left(1 + p\dfrac{1-\eta_0}{1+\eta_0} + pk_{diff}\right) \end{cases} \tag{3.77}$$

Where the function p (depending on the wheel speed difference $\omega_1 - \omega_2$), takes the place of the function $sgn(\Delta\omega)$ to model the gradual transition between $\omega_1 = \omega_2$ and $\omega_1 \neq \omega_2$. Defining the function p as:

$$p = \begin{cases} 1 & \text{for } (\omega_{21} - \omega_{22}) \geq 0{,}2 \\ 5\left|\omega_{21} - \omega_{22}\right| & \text{for } -0{,}2 < (\omega_{21} - \omega_{22}) < 0{,}2 \\ -1 & \text{for } (\omega_{21} - \omega_{22}) \leq -0{,}2 \end{cases} \tag{3.78}$$

the LSD block is able to manage all the differential working conditions. As is possible to note from the Figure 3.3, the p factor represents a very sharp ramp for $-0{,}2 < (\omega_{21} - \omega_{22}) < 0{,}2$; in this way the difference between the simplification introduced in equation (3.77) and $sgn(\Delta\omega)$, is particularly small and is canceled when $|\omega_{21} - \omega_{22}| \geq 0{,}2 rad/s$.

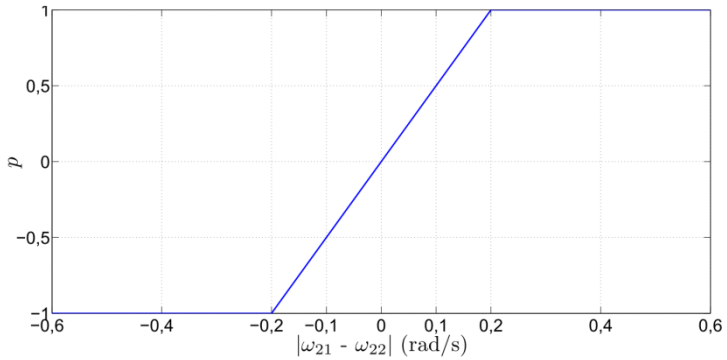

Figure 3.3 - *p* factor

The so characterized differential is of course based on some simplifying hypothesis but has two great advantages: it doesn't introduce any discontinuity nor it limits the kind of possible maneuvers. A similar model of differential has been used by many authors for their work and it always granted excellent results [7].

3.3.7 Firenze Race Team car data: 2708RR model

To validate the Simulink® model of the car it was necessary to have something to confront it with. The basic idea is to make use of the real car the team built for the 2008/2009 season, shown in Figure 3.4, and to obtain all the data needed from the data acquisition system or from some measurements on it.

Figure 3.4 - The 2708RR on Silverstone race track

All the data from the 2708RR have been used both to calibrate the mathematical model and as a control for the results of the simulations. The main data used to calibrate the model are:

- The geometrical and inertial characteristics of the car
- The inertial characteristics, the gear ratio and the efficiency of the driveline system
- The aerodynamic characteristics
- The tyres characteristics.

3.3.7.1 Geometrical and inertial characteristics

All the dimensions, weight and inertial data of the car have been obtained both from the 3D CAD model and from the real car, with appropriate measurements. The CAD also gave all the inertial data of the car, referred to the reference system as described in Chapter 2. The position of the center of mass has been determined using the 3D drawings and, using it, it was possible to determine the static vertical load on tyres. For the whole calculation it was supposed to have an 80kg driver. For what concern aerodynamics, all the data have been obtained from a CFD study performed in the context of the Firenze Race Team activity.

3.3.7.2 Driveline, wheels and tyres characteristics

All the data used for the driveline have been experimentally obtained, measuring the whole system in both dimensions and masses. For the whole driveline chain it was necessary to know the transmission ratio, the efficiency and the inertial characteristics. The locking ratio b of the differential is a known parameter, as the differential itself has been built under Team specifications. The wheels have been characterized both in mass and inertia.

Tyre data are essential for the study done. It was possible to find all the data of the used tyres from the experimental data of the FSAE Tire Test Consortium (FSAE TTC) [8]. The actual tyres mounted on the 2708RR are:

- Front: Avon 6.2/20-13 FITO 9241 Formula SAE Tyre @14psi, 6 inch rim
- Rear: Avon 7.2/20-13 HDTO 9760 Formula SAE Tyre @14psi, 6 inch rim.

All the parameters used to characterize these tyres have been deduced in order to use the PAC2002 formulation of the Pacejka *Magic Formula* [6].

3.3.7.3 Experimental data acquisition

The 2708RR is actually equipped with an 8 channel EVO3 data logging system, able to acquire and record all the engine and car data. With the data logging system mounted on board it's possible to measure all the vehicle center of mass accelerations (lateral, longitudinal and yaw), the wheel rotational velocities, the steering rack position, the throttle valve opening, the engine RPM, and the gas pedal position. All these data are acquired by the data logger and imported in the telemetry software called Racestudio, able to export them in the CSV format (Comma-separated Value). This format is perfect to import them in the Mathlab-Simulink® environment. The data, acquired to use as inputs, are:

- the steering angle
- the engine RPM
- the throttle body valve opening.

The wheels angular velocities and the COG accelerations have been used as reference parameters to test the simulated outputs of the model.

3.4 Simulink® model verification

Two maneuvers have been chosen to test the model: a skid-pad and an acceleration test. The skid-pad test has been conducted as stated by the Formula SAE rules [9], while the acceleration test has been freely performed, just to further test the model. Before starting the two testes, it's opportune to define an absolute reference system $(X, Y, Z; O)$; this system permits to evaluate the vehicle COG trajectory because at the beginning of the run it coincides with the local coordinate system $(x, y, z; G)$ while, during the test, its orientation and position remains constant. The X-Y plane will be the one on which the trajectories will be evaluated, as the Z axis will remain parallel to the z.

3.4.1 Skid-Pad

The layout of the skid-pad test is the one shown in Figure 3.5, and is formed by two couples of coaxial circles, arranged to form an eight shape.

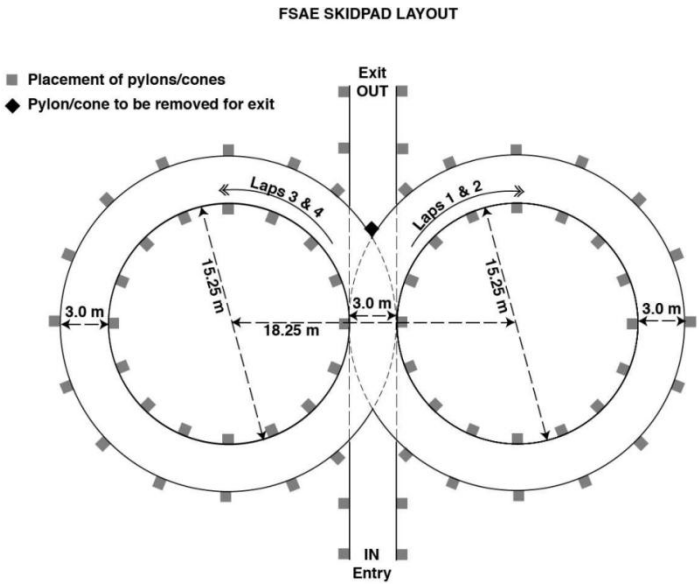

Figure 3.5 - Skid-pad track

The distance between the centers of the circles is 18,25m while the width of the passage (the track) is 3m. The vehicle enters and exits from two three meters wide passages, tangent to the circles, and has to run two laps clockwise and two counterclockwise. To simulate the manoeuvre the steering angle, the throttle

body and the engine RPM during the real test, have been inserted in the Simulink® model thus accurately reproducing the experimental run. It has to be noticed that, in this case, the test is conducted without braking and with a semi-constant speed, so the model limitations are not so hard.

As it's possible to note from Figure 3.6 the run starts with a right steering phase (negative steering angle); the steering angle on the ground rapidly reaches the value of -0,2rad, that are maintained for almost 13 seconds. After a transition phase between the passage from one circle to the other, the steering angle reaches the value of +0,2rad for almost the same time.

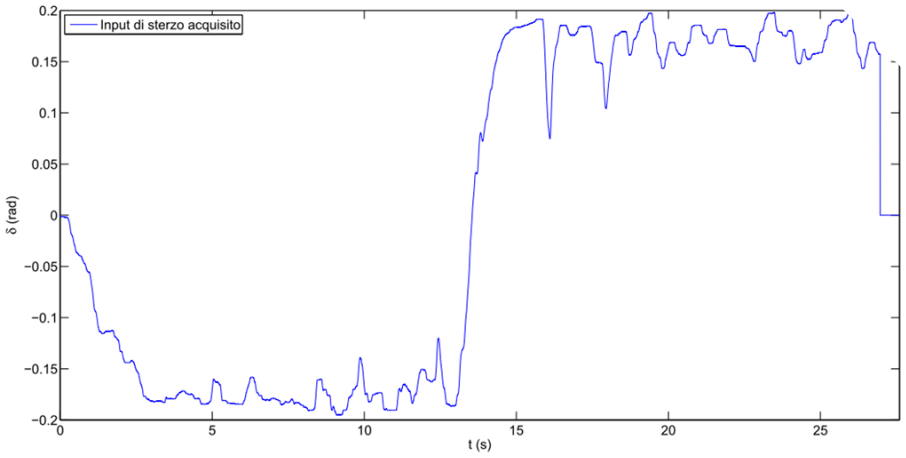

Figure 3.6 - Skid-pad test: steering input

For what concerns the inputs signals that determine the motor torque, visible in Figure 3.7 and Figure 3.8, is possible to note that the driver keeps a 22% opening on the throttle valve and the engine RPM are kept at something around 4000. It's important to note, from the same figures, that no clutch or brakes have been used during the run. As verifying parameters, the two driving wheels speeds and the COG lateral acceleration have been considered. Figure 3.9 shows the velocities of the driving wheel both for the Simulink® model and for the real car: the blue and black one are the acquired real velocities of the 2708RR, while the green and red one are the simulated speeds. The trend is almost the same. The biggest introduced error is noticed across the passage between the clock and the counterclockwise rotation direction as, in this zone, the two rear wheels have the same speed and the differential model introduces the greatest error.

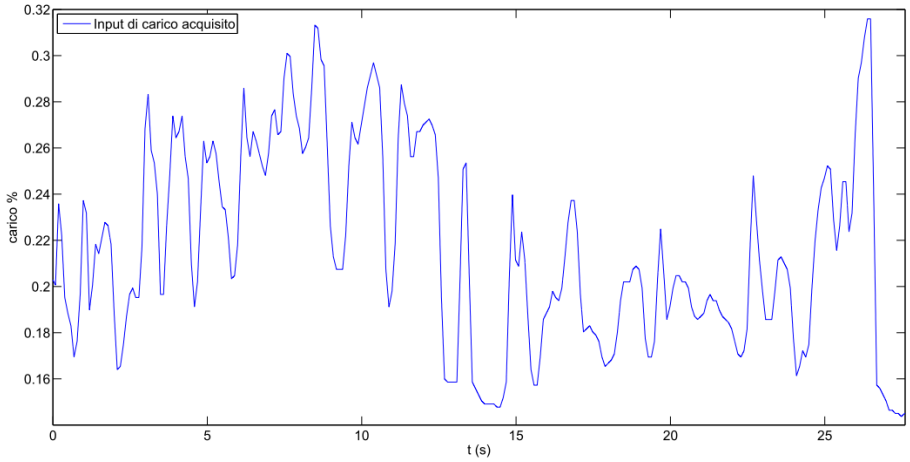

Figure 3.7 - Skid-pad: throttle valve percentage opening

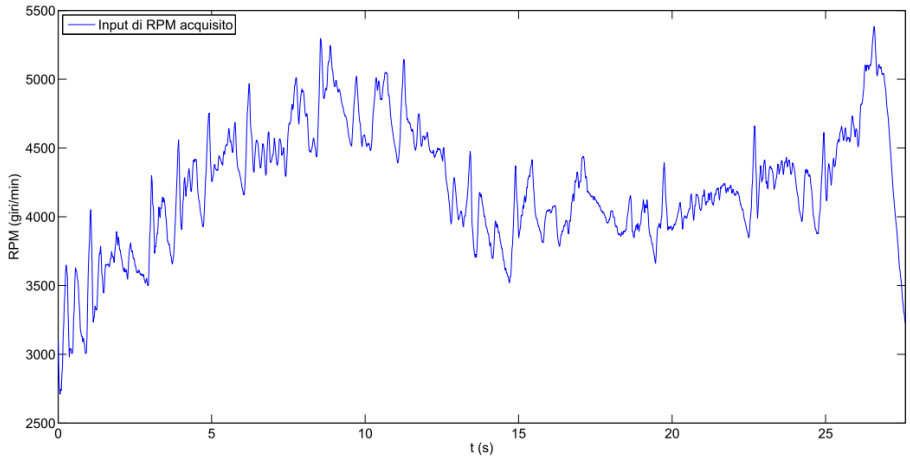

Figure 3.8 - Skid-pad: engine rotational speed input

By the way the greatest error encountered is around 8%, that correspond to a speed difference of $3 \div 4$km/h.

Figure 3.9 also shows that the simulated speeds are always bigger than the acquired ones and these differences increase with the vehicle speed. This difference could be explained by the absence of suspensions, thus by the absence of rolling, pitch and shacking motions of the chassis. For what concerns the center of mass lateral acceleration, as is possible to note in Figure 3.10, the trend is the same, with an error estimable in 10%. This error is probably due to the high sample frequency of the gyrometer, that not only records the lateral accelerations of the COG but also the engine vibrations and other similar background noises.

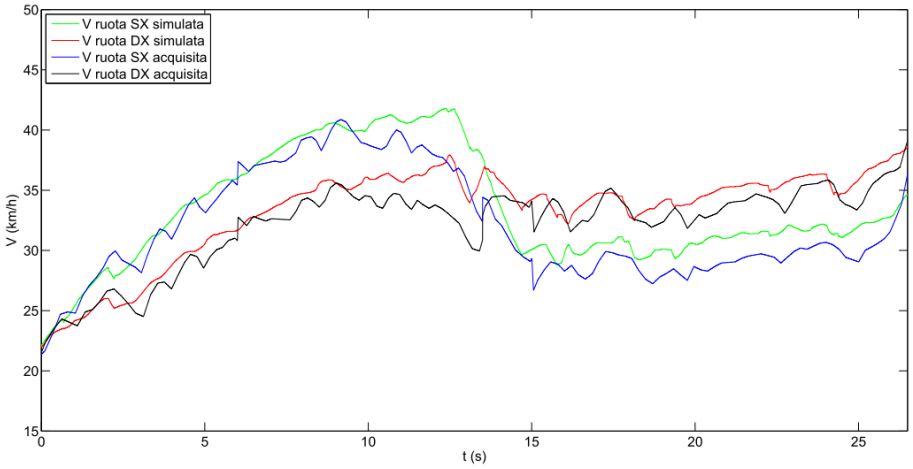

Figure 3.9 - Skid-pad: simulated and experimental driving wheel speeds confrontation

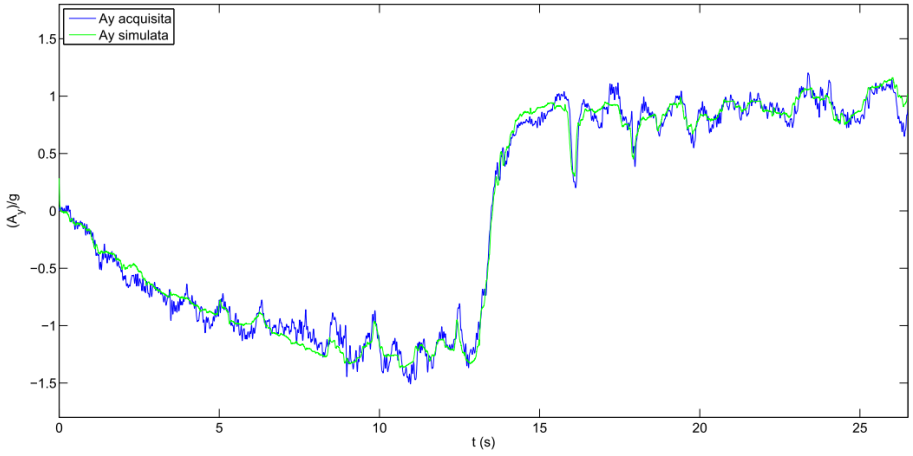

Figure 3.10 - Skid-pad: COG lateral acceleration confrontation

Lastly, Figure 3.11 shows the simulated vehicle trajectory, evaluated in the COG of the car among an absolute reference system. It's really interesting to note that the model perfectly simulates the real run, having the COG a trajectory compatible with the skid-pad track, with a turning radius that let the car staying inside it. As we don't have a GPS system on the car, it's impossible to compare this result with any experimental data. It's now appropriate to verify the hypothesis introduced in chapter 2, using the graphs of Figure 3.12 where is possible to note

that both $\frac{2u}{rt}$ and the ratio $\frac{u}{v}$ are bigger than 10 during the whole test. The almost vertical straight line underline the phases where the trajectory is rectilinear and so characterized by values of r and v, able to let the ratios told before vanish. These results verify the hypothesis that $u \gg \frac{|r|t_1}{2}$ and that $u \gg v$.

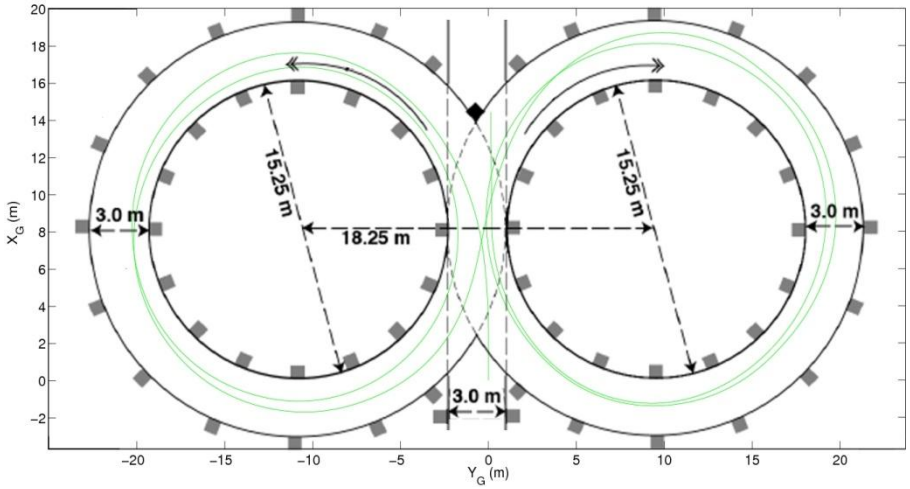

Figure 3.11 - Skid-pad: simulated vehicle trajectory

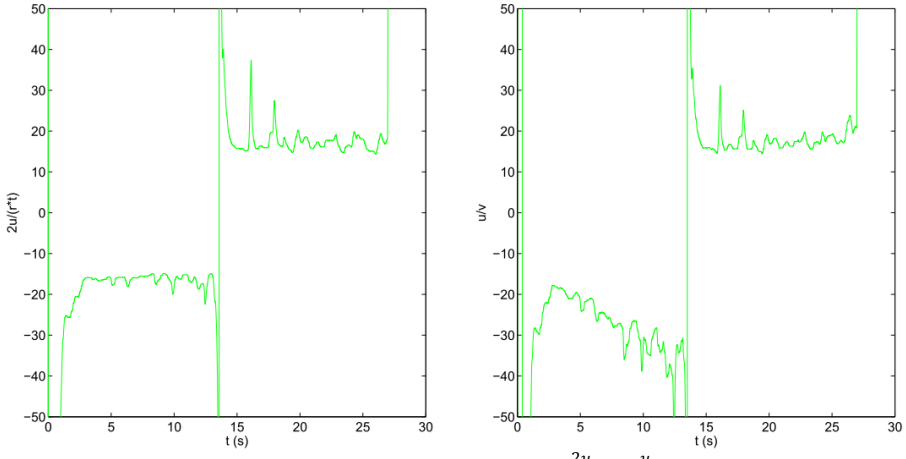

Figure 3.12 - Skid-pad: trend of $\frac{2u}{rt}$ and $\frac{u}{v}$

3.4.2 Acceleration test

This test is developed on the vehicle already running as, not having implemented a clutch on the model, it's impossible to let it start from a still position. It was decided to run a test, both experimental and simulated, where the car accelerates from a speed of approx 20km/h to a speed of 80km/h, with the input data shown in Figure 3.13.

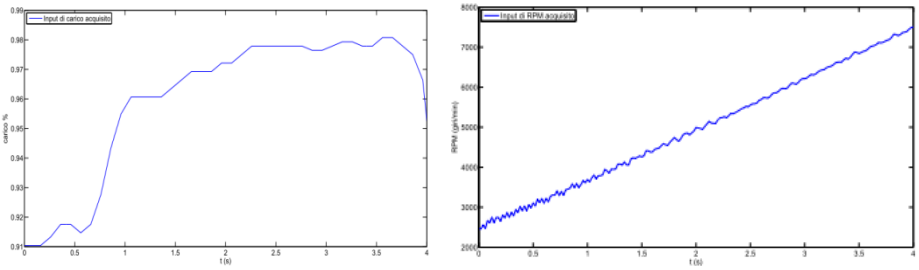

Figure 3.13 - Acceleration test input: throttle valve opening (left) and RPM (right)

The engine RPM increase linearly from 2400 to 7500 in four seconds, while the throttle valve remains at 90-100% of its opening for the whole test. The steering angle is constantly zero.

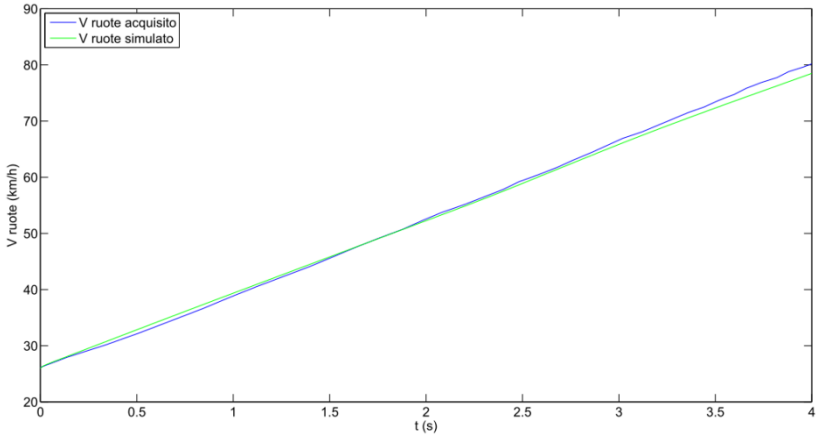

Figure 3.14 - Acceleration test: wheels speed comparison

Figure 3.14 and Figure 3.15 show the result of the test, both for wheel speed and longitudinal acceleration of the COG, compared with the experimental one, acquired on track. In both the graphics the green line represents the simulated value, while the blue one is the experimental one. Again, this test demonstrates

how the model perfectly simulates the behavior of the car, having really small errors (6%).

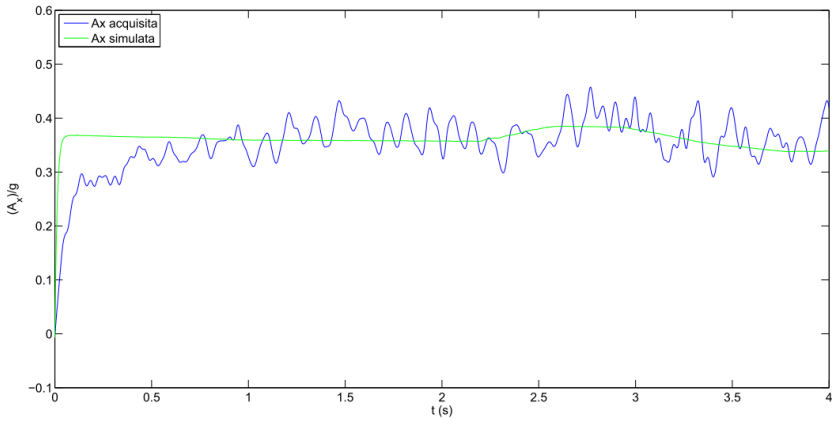

Figure 3.15 - Acceleration test: longitudinal acceleration comparison

After these two testes it's possible to sum, in Table 3-1, the errors of evaluation for the main comparison parameters during the two testes done.

	Wheels speed evaluation error	Acceleration evaluation error
Skid-pad test	8%	10%
Acceleration test	<2%	<6%

Table 3-1 - Evaluation errors

During both testes the approximation obtained with the mathematical model results to be satisfactory, having identified the errors as innate, due to the simplifications introduced. It's now possible to assume the model as being able to model all the dynamic conditions the car could face, so it's possible to use it for the next studies.

3.5 Influence of the differential

In this paragraph the influence of three types of differentials will be analyzed, using the tested Simulink® vehicle model introduced in section 3.3. To reproduce the effects of the different drivelines and to focus only on them, the same "car" is used, only changing the differential system. Using the data of the last Firenze Race Team car a vehicle model has been built and three different kinds of differential have been modeled, in the case in point:

- rigid axle
- open differential
- limited slip differential with a locking ratio of 0,6.

To perform the next testes, the models introduced in chapter 3 have been used, both as been described and modified to have a rigid axle or an open differential. To evaluate how the same turn implies different reactions of the "three vehicles" (namely the same vehicle model equipped with the three differentials) it was decided to simulate the same two maneuver with them all, plotting the results. For both maneuvers (two step-steers) the three vehicles receive, as inputs, the same throttle body valve opening, the same gear, the same RPM and the same steering wheel angle.

3.5.1 Maneuvers description

The two maneuvers used to test the model response are a slow and an high speed step-steer. After a straight part, the car is forced to turn, imposing the same steering angle on the driving wheel and maintaining it for one second.

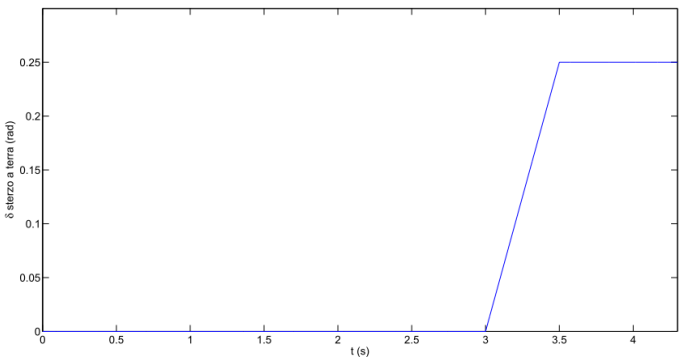

Figure 3.16 - Step-steer steering input

The steering input, as is possible to see in Figure 3.16, is a step signal with a maximum ground steering angle of 0,25rad, having a transitory part of four tenth of second, and being constant for one second. The steering step will be the same for both the step-steers.

The engine RPM and throttle valve opening are different for the two maneuvers and have been taken in order to produce an engine torque of:

- $T_e = 8Nm$ for the slow speed step-steer
- $T_e = 20Nm$ for the high speed step steer.

These two torque values, like the selected gear, remain the same for the whole test duration. The torque values have been chosen to test the model in two different dynamic situations, with different lateral accelerations, so with different load transfers. The results of the tests have been plotted in different colors, to distinguish the three cars: the rigid axle is plotted in black, the open differential in red and the LSD in green.

3.5.2 8Nm step-steer manoeuvre

First of all, it seems to be interesting to comment the different trajectory followed by the three vehicles during the slow step-steer test. To do so, the path of the COG has been plotted, referring to the global reference system $(X, Y, Z; O)$.

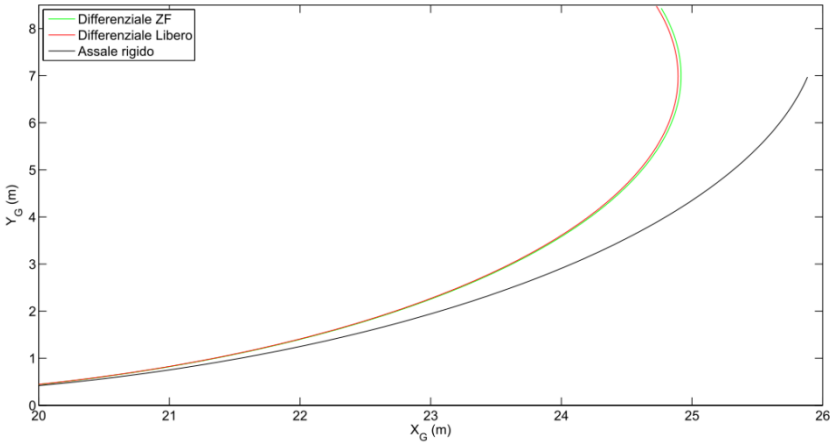

Figure 3.17 - Slow speed step-steer: trajectories

Figure 3.17 shows the distances traveled by the COG, respectively on *Y* and *X* direction. As is possible to note the differential fitted vehicles are able to

maintain the imposed trajectory, while the rigid axle vehicle is not as it cannot properly respond to the steering input. The open differential model results to be able to travel on a narrower path than the LSD model that, on the other hand, introduces an understeering behavior on the vehicle. This behavior is due to the fact that the LSD transfer a bigger torque to the slowest wheel; having only small load transfers, and so small slips, the internal wheel results to be slower and the action of the LSD determines the origin of a yaw moment on the vehicle that opposes to the turn. The open differential, on the other hand, does not introduce this moment. For little motion torque, the small difference between the two trajectories of the open and LS differentials is due to the little torque difference transmitted by the two mechanisms to the wheels. Being the LSD a *torque sensitive* system, when the engine torque is low, it results to be small even the torque displacement ΔT, and it could be compared only to the one due to internal efficiency of an open differential.

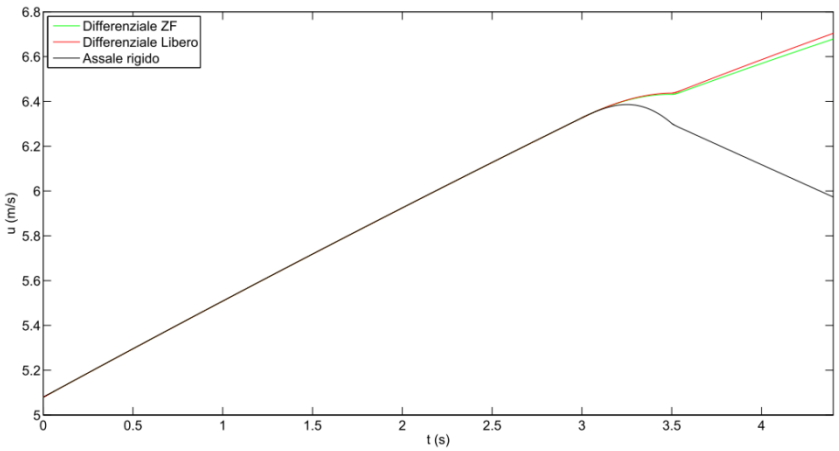

Figure 3.18 – Slow speed step-steer: longitudinal speed

Figure 3.18 shows how rigid axle vehicle longitudinal speed decreases during the turn crossing, while the two other vehicles accelerate. Even having the same torque and RPM inputs, the tyres of the first vehicle, forced to rotate at the same speed, have larger creeps, thus reducing the tangential forces transmitted to the ground. The different way of transmitting the vehicle forces to the ground generates different yaw moments on the car.

Figure 3.19 shows the trend of the yaw moment M_{z_2}; this component is only due to the torque displacement. It's possible to note that an open differential only introduces a small yaw moment, effectively not influencing the car behavior. On the other hand the rigid axle and the LSD differential, for these conditions of low speed and small load transfers, introduce an understeering momentum,

effectively increasing the turning radius. In the case in point the LSD generates a small momentum (about 60Nm), while the rigid axle imposes a huge one (1500Nm) that critically influence the maneuverability of the car.

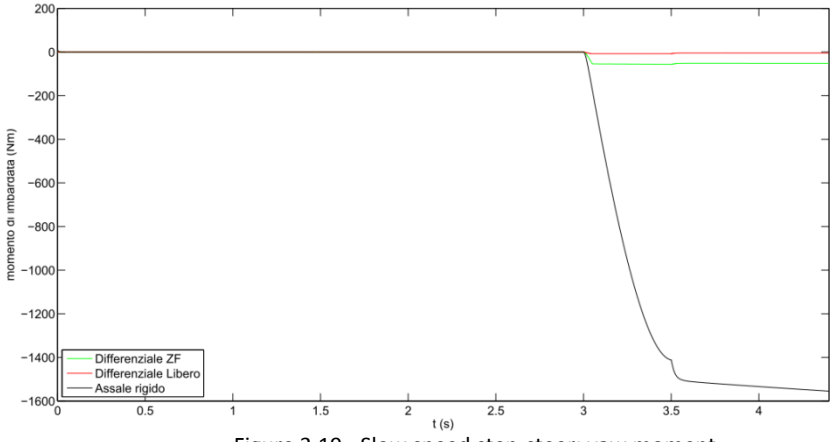

Figure 3.19 - Slow speed step-steer: yaw moment

The presence of an understeering momentum in the rigid axle model implies a reduction of the maximum yaw speed of the order of 0,2rad/s, as shown in Figure 3.20, and, having the same steering angle, a reduction of this speed for every value of δ, compared to the differential fit vehicles, as shown in .

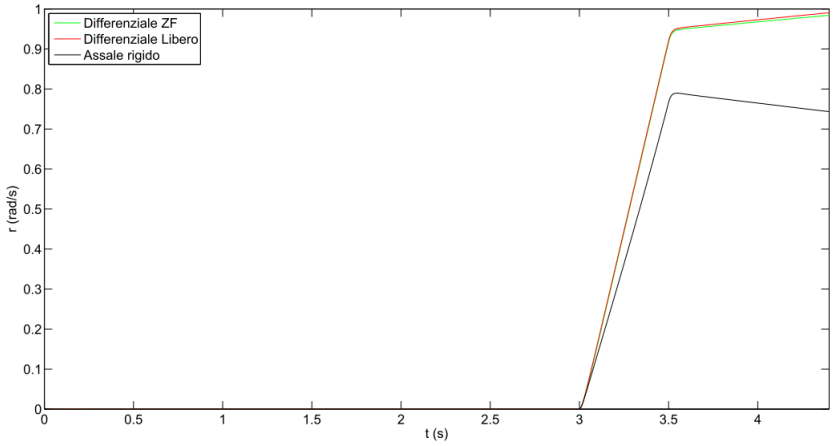

Figure 3.20 - Slow speed step-steer: yaw speed

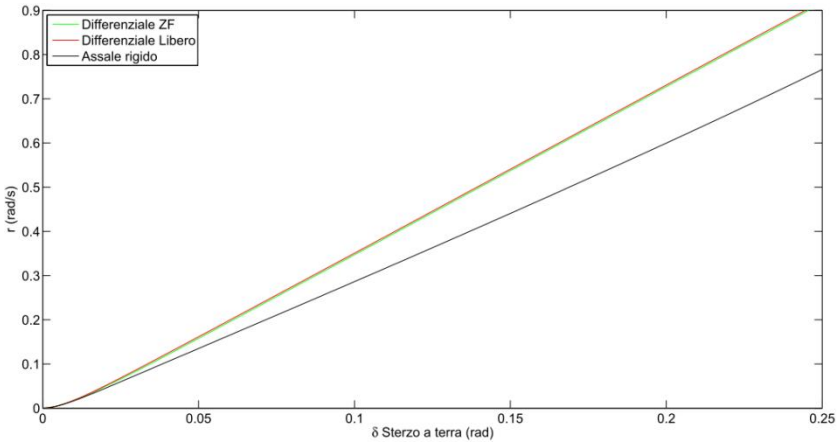

Figure 3.21 - Slow speed step-steer: r as a function of δ

Figure 3.22 shows the torque that the differential transmits to the half shafts: the two differential fit vehicles have different torques on them, while the rigid axle model has the same. The open differential has a torque displacement of about 3Nm, while the LSD has 25Nm. The LSD is able to increase the torque displacement, so it can influence the vehicle handling. For both the vehicles equipped with a differential, is the internal wheel (the left one) that receives the greater torque, being the slowest one (effectively, during the run, both wheels maintain their adherence with ground, as shown), as shown in Figure 3.23.

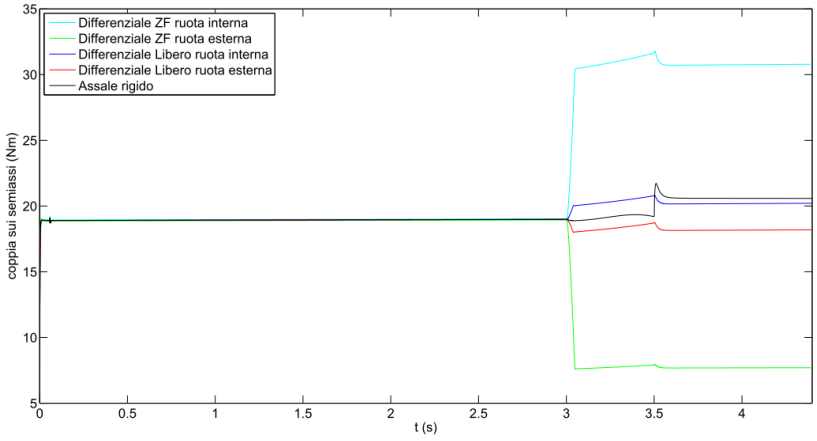

Figure 3.22 - Slow speed step-steer: half shafts torque

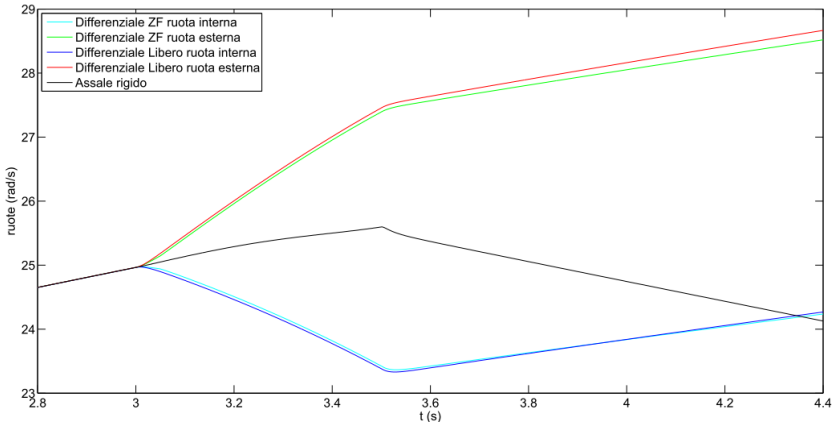

Figure 3.23 - Slow speed step-steer: wheels angular velocities

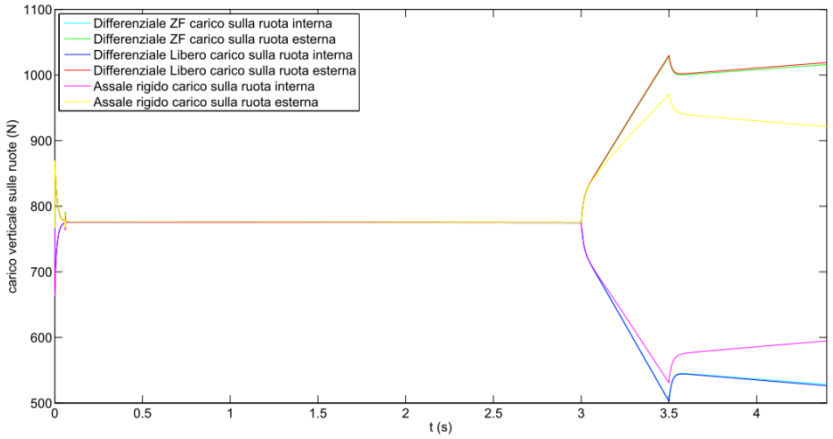

Figure 3.24 - slow speed step-steer: vertical load transfers

Figure 3.24 and Figure 3.25 show the trend of the vertical load transfers and the lateral acceleration of the center of gravity of the cars.

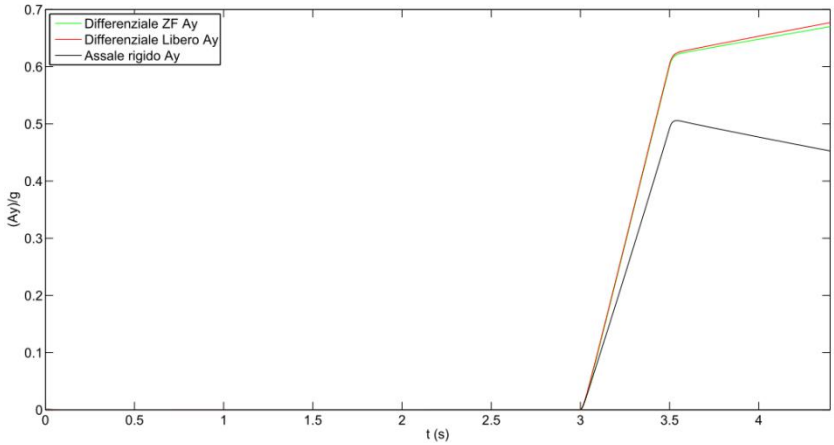

Figure 3.25 - Slow speed step-steer: COG lateral acceleration

3.5.3 20Nm step-steer manoeuvre

Before starting with the results analysis for this test, it is necessary to underline that, increasing the engine torque (so the speed) at which the manoeuvre is dealt, the transient part related to the longer turning increases, thus introducing bigger oscillations of the measured quantities. All the graphs oscillations are imputable to the response of the tyre model to the hard steering and to the behavior of the LSD. It has to be noticed that all these oscillations are mostly located in the final part of the run, where the hypothesis of constant engine torque becomes hard to maintain.

As told before, the steering input remains the same, while the engine torque raises from 8Nm to 20Nm. It's appropriate to start the confrontation of the results from Figure 3.26 and Figure 3.27 where the lateral acceleration and the load transfer between the driving wheels are reported. Until a simulation time $t = 3{,}7s$ these values maintain a limited value, so it's possible to state that the internal wheel, being slower, is subjected to a bigger torque than the external. In this condition the behavior of the LSD and open differential are the same, as the torque displacement is concordant but different in modulus (see Figure 3.28).

With the lateral acceleration increasing, so with the load transfer to the external wheel, the internal tyres reduces its adherence and, event thanks to the greater torque it's receiving, increases its speed. The speeds of the two wheels tend to converge and the torque displacement (related to $\Delta\omega$ by the (3.69)) reduces.

As is possible to note from Figure 3.28 and Figure 3.29, when the wheel speeds converge, the differential inverts the torque transmitted to the half shafts;

doing so it prevents one wheel to improperly accelerate. This effect imply a great asymmetry in torque displacement between the two wheels, so it introduces an understeering effect in the first part of the turn, than an oversteering effect in the second part, when the internal wheel starts to lose adherence with ground.

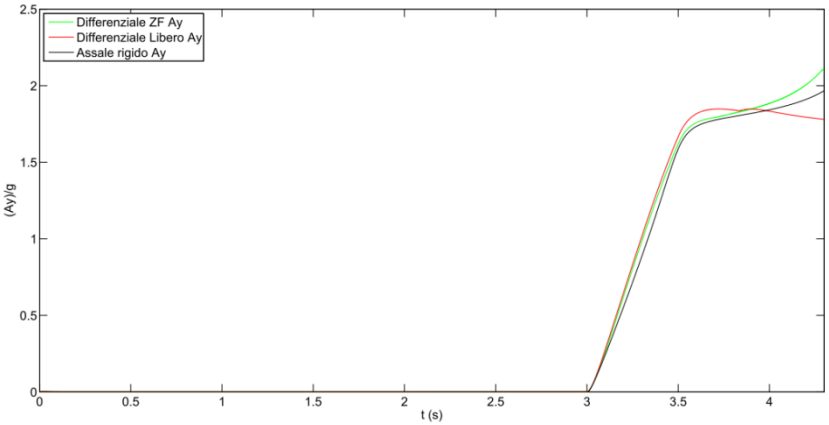

Figure 3.26 - High speed step-steer: lateral acceleration

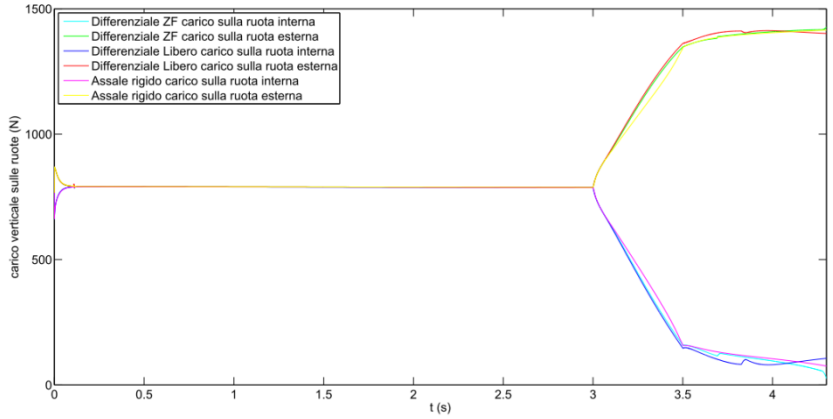

Figure 3.27 - High speed step-steer: vertical load transfer

The open differential transmits an almost identical torque to the half shafts, due to the limited internal frictions and to the poor self locking abilities. That's why the wheels invert their speed: in the first phase of the turn the external wheel is the fastest, while in the second phase it is the internal one, that gradually loses adherence. It's obvious that the rigid axle model only presents one wheel speed and one value of torque.

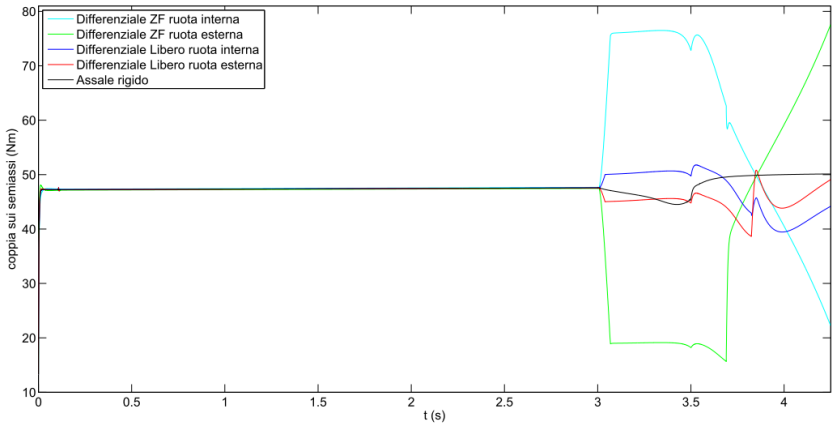

Figure 3.28 - High speed step-steer: half shafts torque

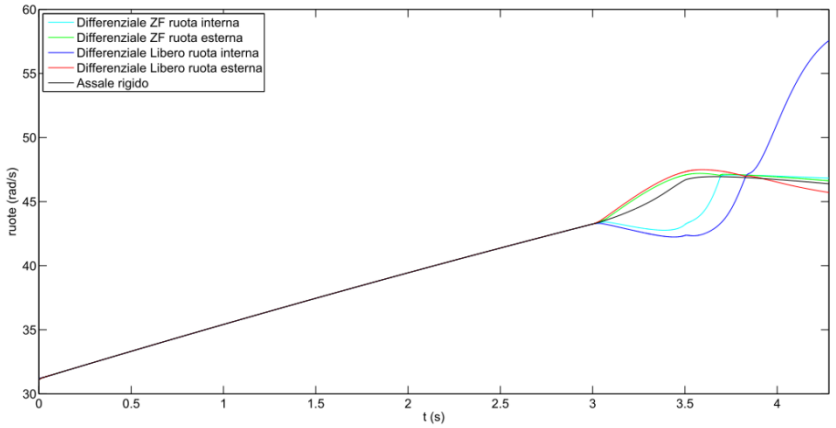

Figure 3.29 - High speed step-steer: wheels angular velocities

The trend of the yaw moment M_{z_2} is plotted in Figure 3.30. As it's possible to note the momentum determined by the open differential results to be neglectable, thus not influencing the vehicle dynamics. On the other hand the contribution to this momentum of both the rigid axle and the LSD appears to be relevant. While $\omega_{21} < \omega_{22}$ both the rigid axle vehicle and the LSD vehicle are subjected to a negative, so understeering, momentum; their turning radius of course, increases. In the moment when, thanks to load transfer, the external wheel starts to receive more torque from the locked differential, the yaw moment become positive and the cars oversteer. It has to be noticed how abrupt is this yaw moment for the rigid axle vehicle: starting from a big negative moment (700Nm) it reduces during the turn covering till becoming positive, so bigger than the one

introduced by the LDS. The progress of M_{z_2} determines an evolution of the yaw speed of the three vehicles, as shown in Figure 3.31. Initially the open differential vehicle results to be the fastest one, even if the differences with the two others are tiny. Starting from the moment in which the internal wheel starts to lose adherence, the two other vehicles manifest a greater speed (with something around 0,4rad), thanks to the oversteering momentum induced by the rigid axle and the LSD.

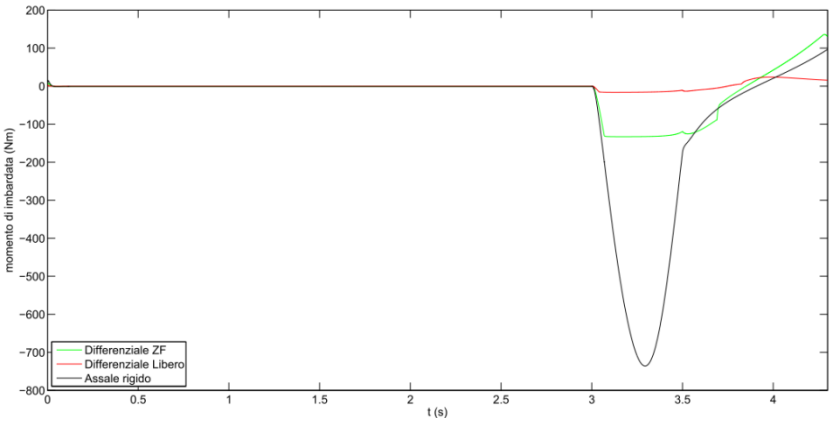

Figure 3.30 - High speed step-steer: yaw moment M_{z_2}

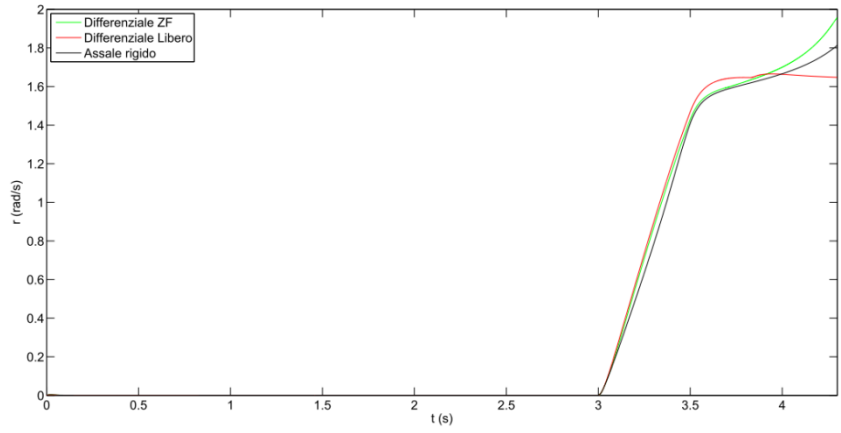

Figure 3.31 - High speed step-steer: yaw speed

Figure 3.32 shows the trajectories followed by the COG of the three vehicles. As it's possible to notice, in the first phase of the turn, the model fitted with the open differential is able to ride the tighter path.

When the external wheel loses adherence and starts to slip, the LSD transmits much more torque on that wheel, so introducing an oversteering moment that helps the vehicle traveling the turn. The rigid axle model manifest a more understeering behavior in the first phase, and assumes an oversteering behavior in the second phase.

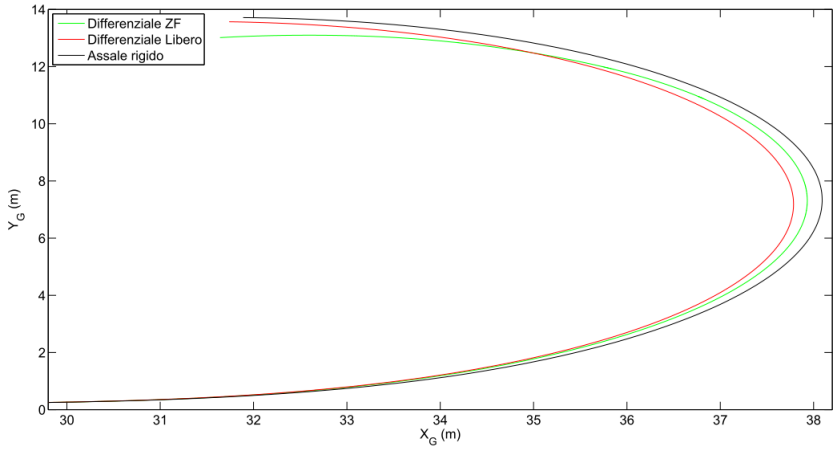

Figure 3.32 - High speed step-steer: trajectories

Figure 3.33 shows the longitudinal speed of the three models: it is possible to note how the behavior of this dimension is almost the same for all the models.

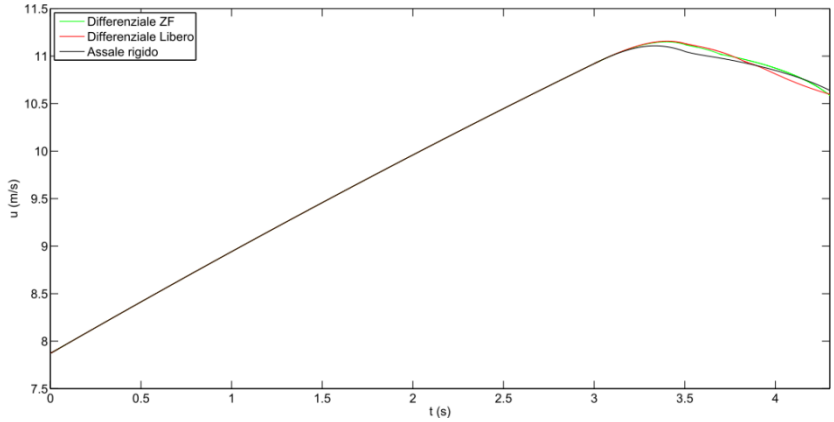

Figure 3.33 - High speed step-steer: longitudinal speed

3.5.4 Comments on the step-steer tests

Thanks to the two tests it was possible to analyze the behavior of a vehicle fit with a differential and to study the influence it has on the vehicle handling. It's evident how, both at slow or high speed, this mechanism is necessary.

For what concern a Formula SAE cars, being judged during events especially for its handling and maneuverability on tracks, it's fundamental to equip it with a well calibrated differential, despite the evident increase of weight of the car and, of course, cost.

Another note has to be done on the LSD differential. Even if, at slow speed, the differences with the open differential are small and neglectable, at high speed it manifested some interesting advantages, like:

- ability to modify vehicle handling in terms of under-oversteering
- ability to divide the engine torque on the two half shafts asymmetrically, so granting a larger traction
- higher yaw speed, effectively granting tighter trajectories.

All these advantages confirmed the choice of equipping the Firenze Race Team cars with an LSD instead of an open differential. It's also interesting to note how, using an LSD, is possible to modify the vehicle behavior on the different tests the car has to face, varying the torque distribution on the half shafts. It's now necessary to analyze how an LSD modifies the vehicle handling and how its locking ratio influences the car's behavior.

3.6 LSD and locking ratio analysis

The tangential forces that a tyre exchanges with the ground influence the dynamic behavior of a vehicle and are dependent from the tyres characteristics themselves and from the rolling conditions determined by the torque balance on the wheel. The vehicle handling results very influenced by some designing parameters, like suspension's parameters, and from the way the engine torque is divided on wheels by the driveline. Some parameters are defined during the design process of the vehicle and cannot be modified during the future "life" of the car: it's easy to understand how a rear-wheel drive car has a different behavior than a front-wheel drive car and it's almost impossible to convert a kind from one system to the other.

Once the driveline configuration has been decided, it's likewise quite easy to set up the differential with different locking ratios and, so, modify the vehicle behavior.

For race cars, like the 2708RR, the differential set up strongly modifies both the release phase in turn entrance and the acceleration phase in turn exit. All the Firenze Race Team cars have been equipped with a limited slip differential that mechanically divide the engine torque on the half shafts. This kind of differential divides the engine torque on the wheels as stated by equations (3.68), once the locking ratio has been set (modifying the ramp inclinations and the number of friction discs). Of course these modifications cannot be done on the fly during a run, and it's so necessary to find a good compromise for the setup to have a car that can adapt to the difference conditions of a race.

Of course, to reach the best performances on track, it's always desirable to overcome this limitation, and have a car that can vary its behavior as a function of the turn it's crossing. A great help, in this sense, could come from the electro-actuated limited slip differential that, thanks to a control system, varies it's behavior and "refresh" the response of the mechanical system as a function of the external variables. This paragraph is intended as a study on the influence that the locking ratio has on the differential and on its effects on the vehicle dynamics.

3.6.1 Tests definition

To prove the influence of the differential and the locking ratio on the car behavior, it has been decided to run a common maneuver, of course involving a turn. After a straight part the vehicle enters a turn with a fast steering transitory, than it goes through the entire curve maintaining the same steering angle, to finally exit with a similar maneuver. To develop this analysis it was decided to improve two different kind of maneuvers:

- A left turn with a big turning radius, travelled at high speed with a step steer of 1s, with a steering angle of 0,3rad
- A left turn with a small turning radius, travelled at slow speed with a step steer of 1s, with a steering angle of 0,14rad.

These two kinds of turns have been chosen after an analysis of the 2708RR telemetry, recorded during the last Formula Student race, as they seem to be the most common turning conditions on track. For both the turns, three different locking ratios b have been tested, to evaluate the influence of the differential on the vehicle behavior. These three ratios represent the actual setup of the differential and a variation from it of $\pm 30\%$.

3.6.2 Large turning radius

During this test, the model inputs are:

- A constant engine torque of 24Nm
- the use of the fourth gear
- the steering signal as in Figure 3.34.

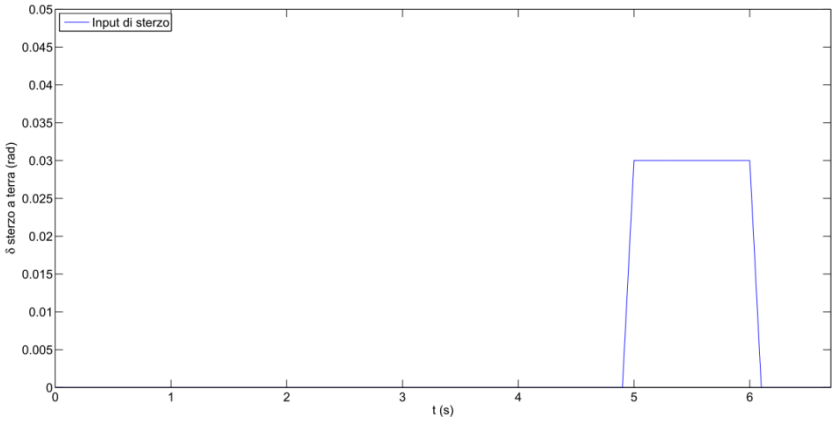

Figure 3.34 - Large turning radius: steering input

This run is characterized by a lateral acceleration, a_y, lower than 1g, as shown in Figure 3.35, that is almost the one registered during the skid-pad test; with these values of a_y the load transfer on the two driving wheel is 300N (Figure 3.36).

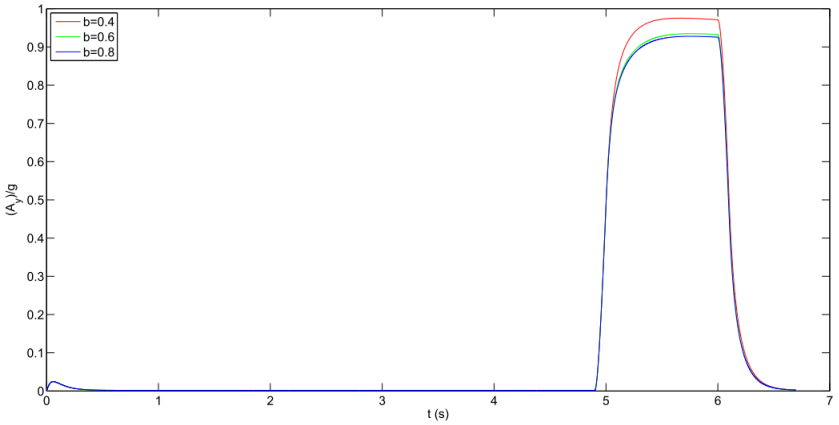

Figure 3.35 - Large turning radius: COG lateral acceleration

As shown in Figure 3.37, none of the "three" differentials reach the locking conditions; it effectively results that the condition $\omega_{21} = \omega_{22}$ is reached only before and after the turn. The wheel speeds diverges at the moment in which the car enters the turn and it's possible to note how, with a greater locking ratio of the differential, the difference between ω_{21} and ω_{22} decreases. The speeds uniformly decreases during the constant turning phase and tend to converge during the turning exit.

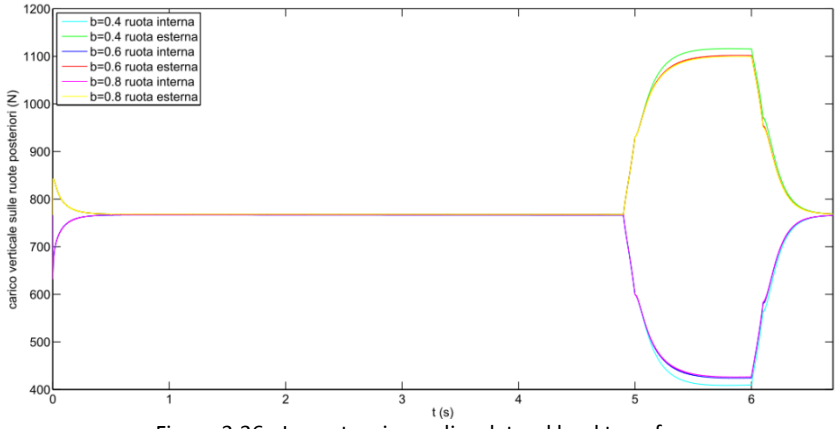

Figure 3.36 - Large turning radius: lateral load transfer

The vehicle with $b = 0{,}4$ results to have a rear wheel speed lower than the others. It's also possible to note that the maximum $\Delta\omega$ is reached, for all the vehicles, at the same instant at the end of the steering unsteady state. This

condition coincides with the achievement of the maximum torque displacement on the half shafts, as shown in Figure 3.38.

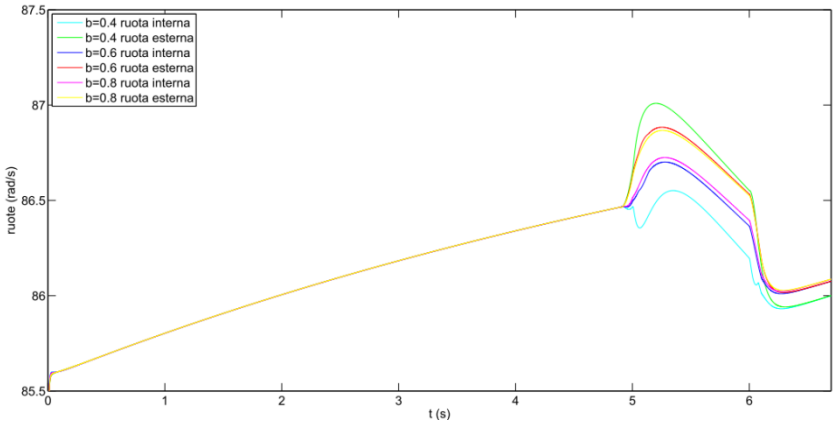

Figure 3.37 - Large turning radius: wheel angular velocity

The torque displacement $\Delta C = T_{22} - T_{21}$, according to (3.70), is proportional to the torque entering the differential (considered to be constant); ΔC varies for the three vehicles as a function of b and is 70N for b=0,8, 65N for b=0,6 and 40N for b=0,4.

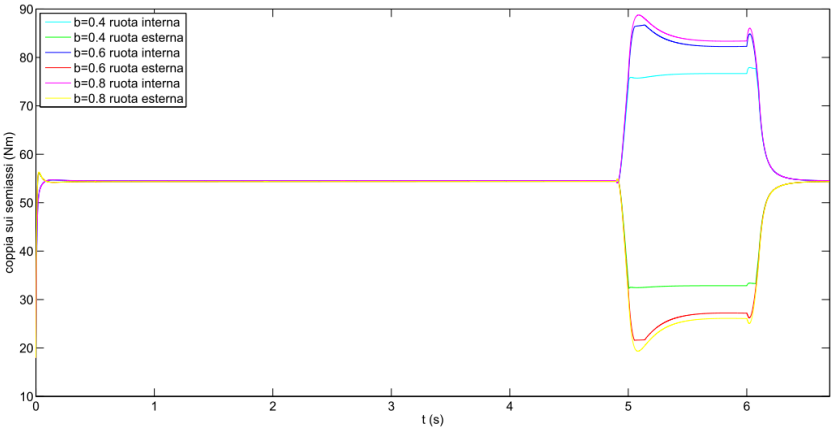

Figure 3.38 - Large turning radius: motor torque to wheels

Of course this torque displacement produces some longitudinal forces that generate a negative, so understeering, yaw moment M_{z_2} for all the vehicles. From an analysis of the Figure 3.39 and Figure 3.40 it's possible to note that, in these conditions, a vehicle fit with a less locked differential results to have smaller

values of M_{z_2}, so bigger yaw speed *r*. In the case of this test the car with $b = 0{,}4$ has a yaw moment 50Nm lower than the two others, so a value of *r*, larger for 0,05rad/s.

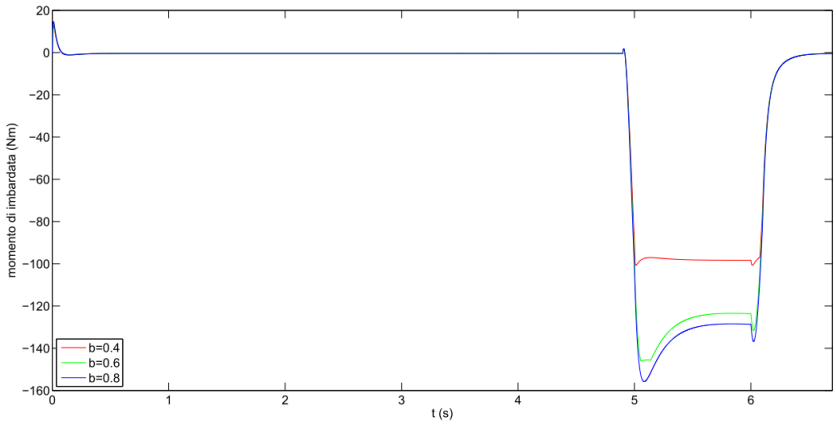

Figure 3.39 - Large turning radius: yaw moment M_{z_2}

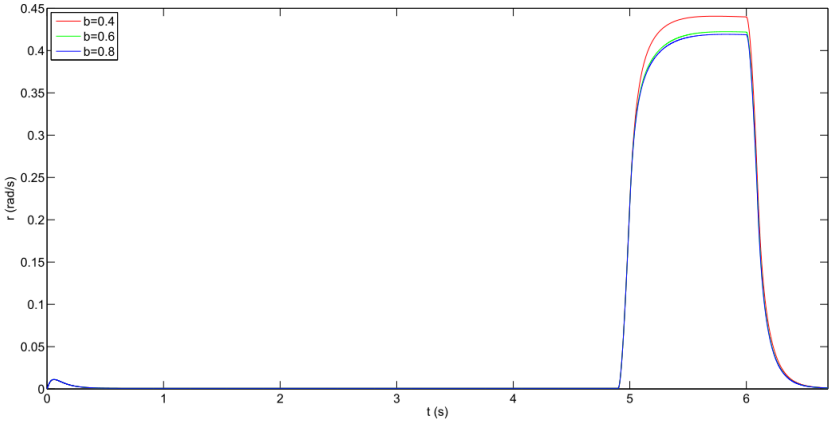

Figure 3.40 - Large turning radius: yaw speed

Figure 3.41 and Figure 3.42 show the trend of the COG trajectory referring to an absolute reference system $(X, Y, Z; O)$ and the corresponding turning radius. The vehicle with $b = 0{,}4$ travels on a turn 3m smaller than the others. It's also possible to note how the longitudinal component *u* of the wheels speed of the same $b = 0{,}4$ vehicle, is smaller than the others.

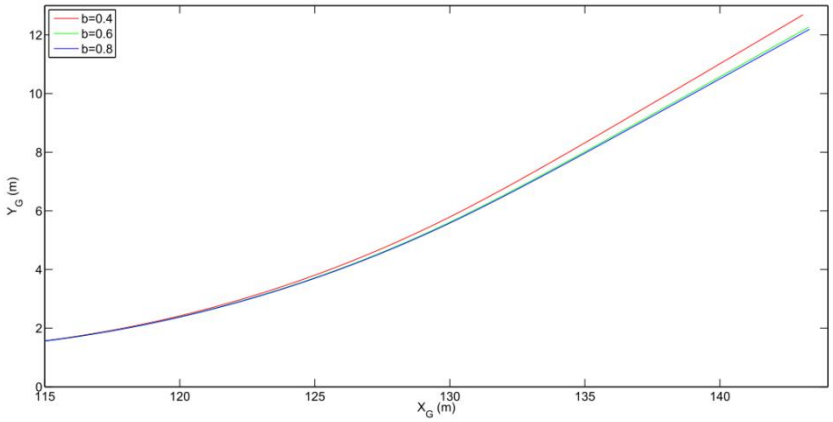

Figure 3.41 - Large turning radius: COG trajectory

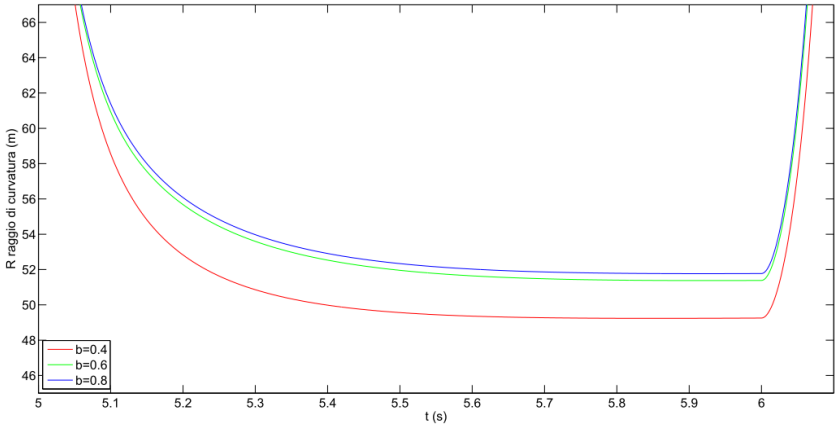

Figure 3.42 - Large turning radius: turning radius

3.6.3 Small turning radius

The aim of this test is to reach, during the turning covering, values of lateral accelerations able to lighten the internal wheel until locking conditions. For this reason it was decided to simulate a turn as narrow as the Formula SAE rules allow. For what concern the input conditions of the test, they are:

- A constant engine torque of 12Nm
- the use of the second gear
- the steering signal as in Figure 3.43

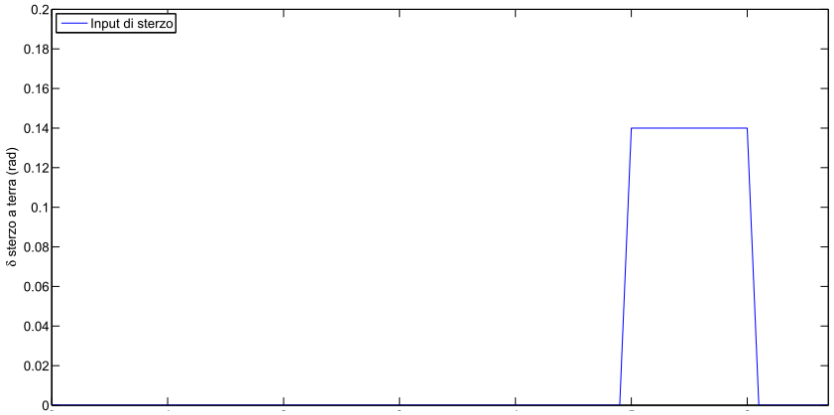

Figure 3.43 - Small turning radius: steering input

The steering input is the same of the previous test, except for the maximum value. The lateral acceleration, as shown in Figure 3.44, reaches, at the end of the unsteady state steering phase, a value close to 1,85g and tends to increase during turning. In this phase the difference between the three vehicles yet results evident. Figure 3.44 shows how the differential locking influences the vehicle behavior: during turn covering, a greater value of *b* determines a greater lateral acceleration, due to the generation of oversteering moments.

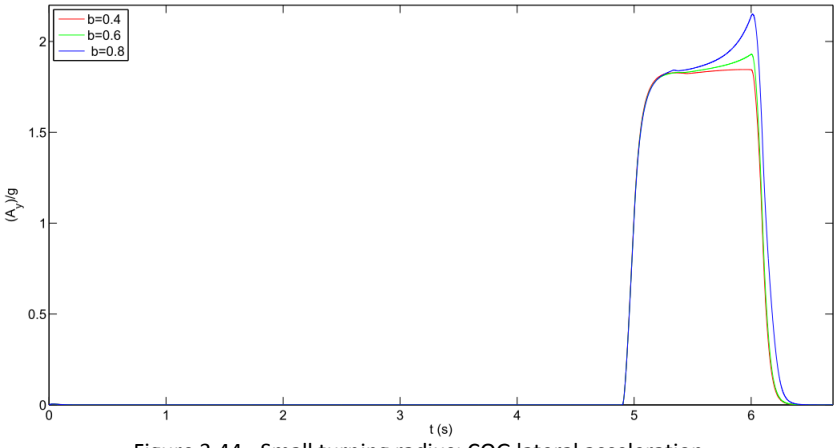

Figure 3.44 - Small turning radius: COG lateral acceleration

Load transfer, shown in Figure 3.45, is able to induce a great lightening of the internal wheel that, losing adherence, determines the locking of the differential for all the values of *b*.

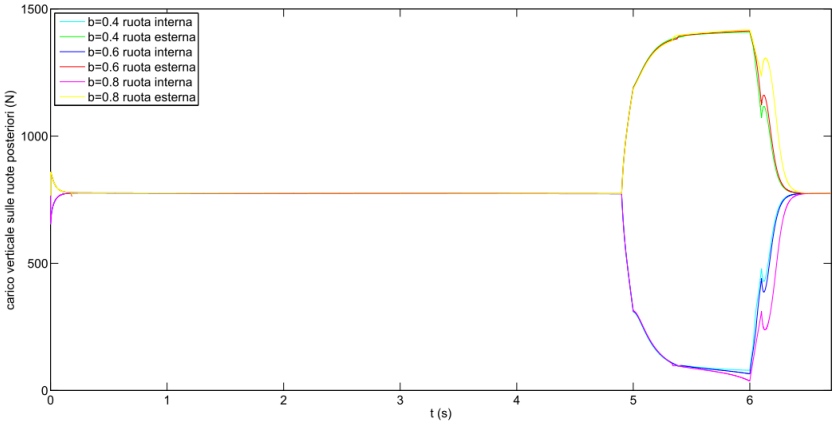

Figure 3.45 - Small turning radius: lateral load transfer

From Figure 3.46 and Figure 3.47 is possible to note how, during the first part of the turn, the external wheel rotates at higher speed, so it receives less torque than the internal. The combined effect of this torque asymmetry and the load transfer to the external wheel, produce a speed increase of the internal wheel up to the condition of $\omega_{21} = \omega_{22}$. Once this condition is reached, the LSDs invert the torque distributed to the half shafts, preventing the internal one to over-accelerate and maintaining the two wheels at the same speed.

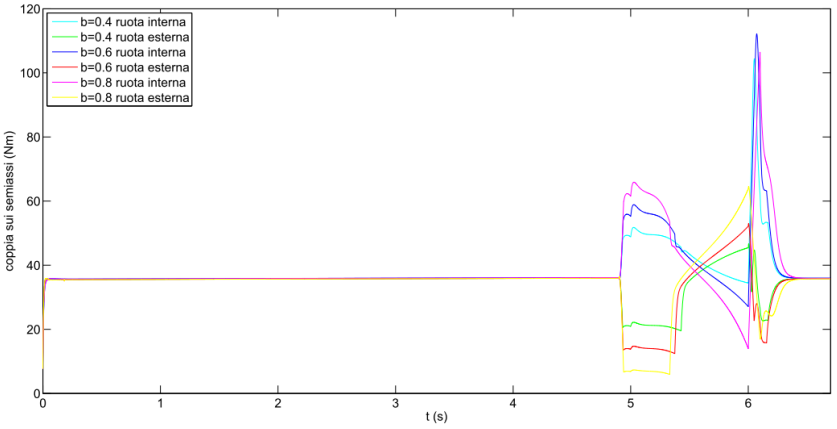

Figure 3.46 - Small turning radius: motor torque on wheels

At $t = 6s$ the steering angle starts to decrease: the load on the wheel begun to go back to the static values so the internal wheel slows down, determining the unlocking of the differential. The wheel speeds are now the same, being the vehicle in the straight part of the run.

Analyzing in detail the difference of performance of the three differentials is possible to note that, increasing *b*, there is a bigger displacement of torque between the half shafts and a smaller difference of rotating speed between them; the locking condition is so quickly reached. In this condition the LSD allow the external wheel to transmit bigger longitudinal forces, so traction of the vehicle is increased.

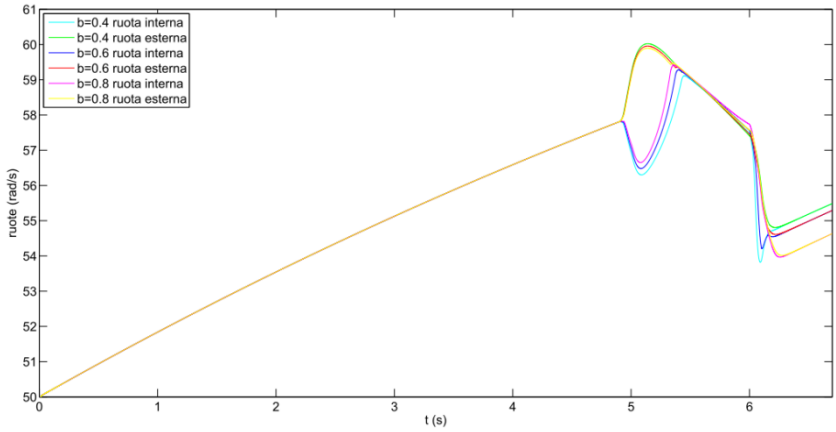

Figure 3.47 - Small turning radius: wheels angular velocity

The last statement is confirmed by Figure 3.48 where is possible to note that, during the first part of the turn, M_{z_2} results negative than it becomes positive once the locking conditions are reached.

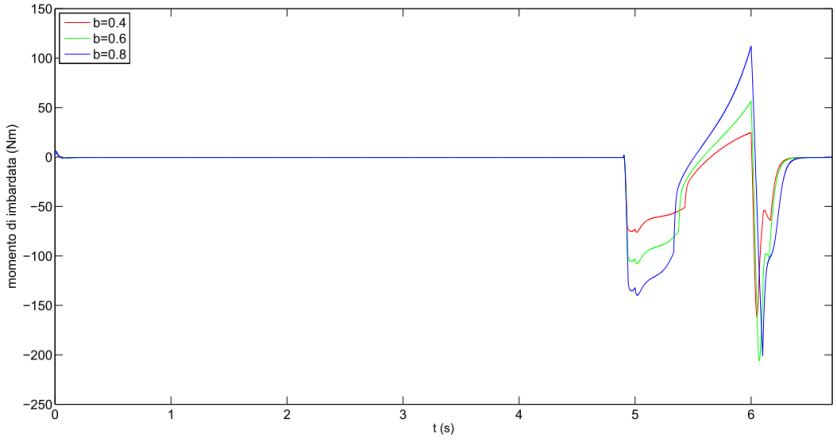

Figure 3.48 - Small turning radius: yaw moment M_{z_2}

In these conditions the differential with $b = 0{,}4$ does not give an oversteering moment during the turning covering, so not granting the driver a help in "closing" the turn. The differential with $b = 0{,}8$, on the other hand, determines an oversteering moment of about 100Nm but also an understeering moment in the first part of the turn. The actual LSD that is mounted on the 2708RR results to be a compromise between these two solutions, giving an oversteering moment of 50Nm and an understeering moment of 100Nm.

As is possible to note from Figure 3.49, only in the case of $b = 0{,}8$ the vehicle get over $1{,}5 rad/s$ while in the other cases r reaches values around $1{,}35 rad/s$.

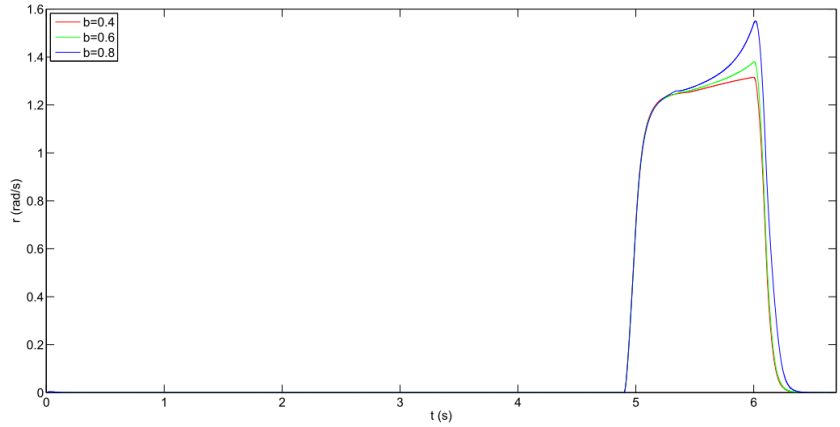

Figure 3.49 - Small turning radius: yaw speed

Analyzing Figure 3.50 and Figure 3.51 it's possible to note that the vehicle fit with the most locked differential, in the second phase of the turn, tends to "close" the trajectory, reducing the turning radius, thus going into an instability condition (like, for instance, spinning right round).

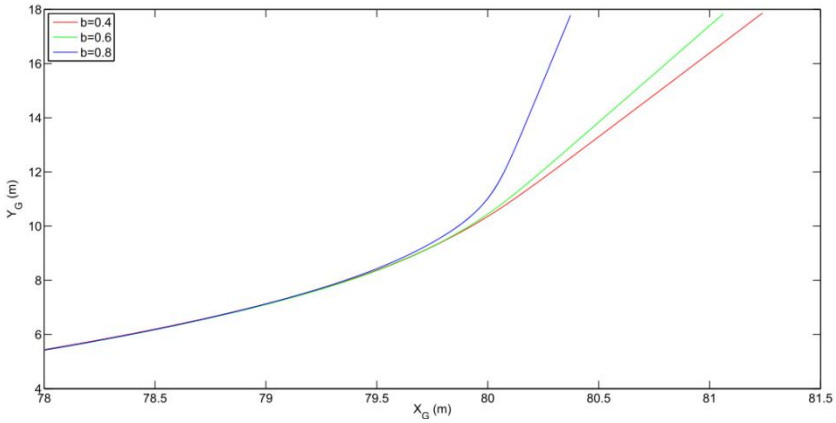

Figure 3.50 - Small turning radius: trajectories

This thing can be confirmed looking at Figure 3.51, where the vehicle with $b = 0{,}8$ continue to reduce its turning radius, despite the reduction of the steering angle on ground, while the two other vehicles increase it, going back to a straight motion.

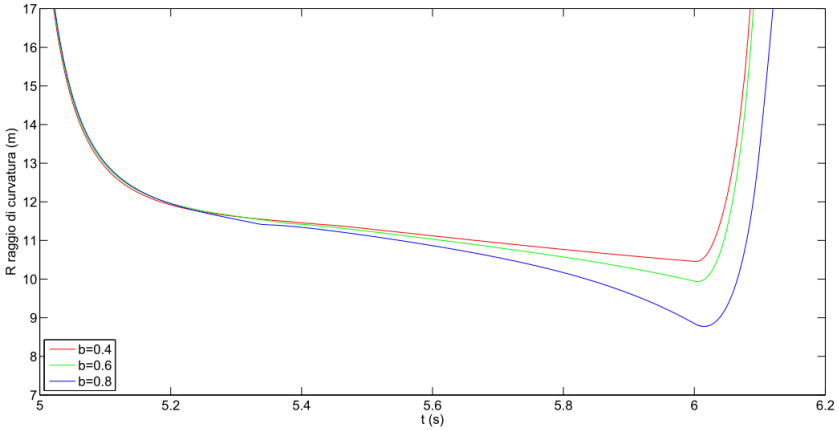

Figure 3.51 - Small turning radius: turning radius

In the end, Figure 3.51 Figure 3.52, shows the trend of the longitudinal component of the vehicle speed. Coherently with Figure 3.47 the vehicle with the greater locking ratio travels and exits the turn with the lowest *u* component, due to the bigger yaw speed.

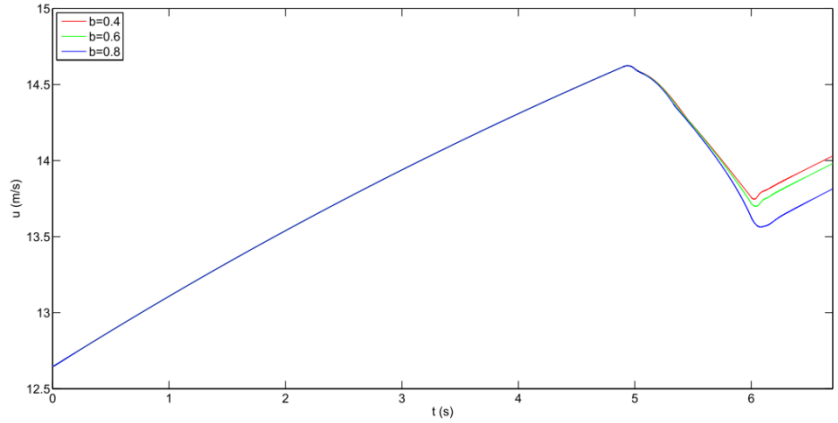

Figure 3.52 - Small turning radius: longitudinal speed

3.6.4 Comments on LSD locking ratio

From all the analysis done, it's easy to understand how the differential locking ratio *b*, influences the vehicle behavior, as it generates a yaw moment dependent from the torque displacement. With the LSD the motor torque displacement is dependent from the engine torque, the ratio *b* and from the running condition during turning, in particular lateral acceleration and load transfer. All the simulation have been conduced maintaining a constant engine torque, in order to suppress a degree of freedom and focus on the influence of *b* on the vehicle behavior.

It's interesting to notice how, having values of the lateral acceleration lower than the one reached during the skid-pad test, locking condition are not reached neither from the actual 2708RR differential nor from the one with *b* increased by 30%. In this condition the vehicle results to be constantly understeering and increasing the locking ratio would only worsen this situation. It could even be useful to reduce the internal friction coefficient, in order to reduce the influence of the differential on the turn. Reaching large lateral accelerations and reaching locking conditions, the LSD differential generates an oversteering moment. This moment results to be dependent, more than from the engine torque, from the parameter *b*.

In the same conditions a more locked differential implies a larger oversteering moment that could be interpreted as an help in turning, allowing narrower turns, but this moment could be dangerous in case it reaches excessive values, inducing instabilities in vehicle motion.

In case the vehicle is requested to face different kind of turns or maneuvers, it's impossible to determine an optimal setting for the differential, also

fitting all the different driving styles. With an LSD it's so necessary to find a compromise for the value of *b*, or to use an electronic LSD.

An electronic, or active, differential could varies its locking ratio as a function of the travelled turn, effectively reducing the under or oversteering behavior of the car during corners entering, travelling and exiting.

4 15 DOF vehicle model

4.1 Introduction to the model

As previously seen the 3 DOF model was really useful to understand the basic dynamic behavior of a Formula SAE car under some driving conditions. In particular the model excellently reproduce the vehicle behavior during some maneuvers like cornering and turn entering and exit.

Thanks to the way it has been modeled, namely using all the exact geometric and inertial data of Firenze Race Team last car, the model perfectly reproduce the behavior of it, especially simulating the influence on its dynamic of the differential. Again the model has been used to simulate diverse kind of differentials, and different locking ratio for the LSD, in order to deeply analyze the influence of this component on the vehicle handling. It was so possible to have a first knowledge of the basic parameters that contribute to the handling of the car and to its stability during critical maneuver like turns and skid-pads.

Even if the indications provided by such a model are interesting and particularly useful to start a dynamic analysis on the car, they have some lacks for what concern the chassis accelerations and for the suspensions behavior during travelling. It resulted necessary to think at another way of modeling the car, introducing much more degrees of freedom, especially for what concerns suspensions, wheels and chassis motions.

To effectively model the vehicle with all the elastic parts implemented, it was necessary, of course, to introduce all the motions of the chassis and relate them to the motions of the suspensions. The degrees of freedom are now increased, as the vehicle is no more considered to be a rigid body on a plane surface, but as a series of attached bodies, put on an irregular road. Starting from the chassis, that has six DOF, all the suspensions have been modeled, adding four more DOF (vertical motion of the suspension) and the same for the wheels, with four more DOF. The fifteenth degree is represented by the steering of the front wheels. A model so defined is able to perform almost all the driving condition a Formula SAE car could face on track, and is also able to respond properly to road

inputs, giving as outputs all the chassis accelerations (longitudinal, lateral, yaw, roll, etc.) and forces on tyres and, so, suspensions.

Again, for this model, it was necessary to introduce some simplifications, due to the large amount of formulae needed to schematize the system and to the intrinsic complexity of the motions. It has to be noticed that:

- All the bonds are ideal, with no friction
- Air resistance has been neglected
- The chassis has been supposed to be totally rigid
- The single suspension parts (i.e. the arms) have been supposed totally rigid.

It has to be noticed that the wheels have been modeled using two elements, one for the upright and one for the wheel (including the tyre and the rim), all considered to be rigid. The vehicle motion is studied always referring to an inertial reference system, united to the ground, that is the one of greatest engineering interest.

The system receives, as inputs, the engine torque and the interaction forces between road and tyre: in this way it's possible to represent a sort of "poster rig" effectively reproducing all possible road conditions. As output the system gives the position, speed and acceleration of the chassis COG, the values of the roll, yaw and pitch angles and the angular speed and acceleration of the chassis.

To build this model it was decide to adopt two different Matlab® libraries, in particular Simulink® and SimMechanics®. Even these two libraries look very similar, they have some great differences. If a Simulink® diagram represent a mathematical operation, or group of operations, a SimMechanics® block represents directly the physic of the object it is modeling, in terms of inertia, mass and kinematic links with the other components of the system. It has to be noticed that SimMechanics® is not independent from Simulink®, as the block of the first are effectively modeled using the second. Simulink® is also used to produce the data tables necessary to let the model work. Even if it could be possible to build the model directly using Simulink®, it was decided to use SimMechanics® for some motivations:

- The possibility of having a model with less blocks
- The possibility to have, as output, not only the graphs of the interesting dimensions, but also a 3D visualization of the vehicle
- The easier way the model is represented that let an observer understand

- The more practicality for a future development or modification of the model.

In this model SimMechanics® has been used to model the chassis, the suspensions, the uprights, the tyres and the links between all these elements and the simulating ambient.

On the other hand, Simulink®, has been used to model the ground-tyre contact, to introduce the engine torque data and to actuate the model with the interaction forces between road and tyre.

4.2 Model structure

The model is essentially made of five parts:

- The simulation environment
- The chassis
- The suspensions
- The wheels
- The actuation blocks.

To make the comprehension of the model easy it was decided to refer to a color scheme, in order to regroup all the symmetrical components and the blocks that, together, are used to model an element of the vehicle. The colors are the ones reported in Table 4-1.

Color	Description
Orange	Ground, simulation environment and road-wheel contact blocks
Yellow	Chassis
Red	Calculating blocks that provide graphs as a function of time
Dark green	Lower suspensions arms
Light green	Upper suspensions arms
Turquoise	Suspensions tracks
Water green	Push, Rocker, dampers and springs
Blue	Uprights, wheel rim and tyres
Violet and purple	Actuating blocks

Table 4-1 - Color scheme

Figure 4.1 shows the complete SimMechanics® model. Each block has a different name and is followed by a number and a letter. Number 1 refers to the front blocks, while number 2 refers to rear blocks. The *s* letter refers to the left side of the car, while the *d* refers to the right side.

The model environment is defined by two orange blocks, as shown in Figure 4.2: the *Ground* block and the *Machine Environment* block. It has to be noticed that, in SimMechanics®, the term *machine* refers to a completely independent blocks diagram that can move independently from every other system present in the model. Each *machine* to be defined, needs the two previously introduced blocks, *Ground* and *Machine Environment*.

The *Ground* block represents an inertial reference system to which a right-side Cartesian Coordinate System (CS) is associated, having the *z* axis vertical and upward. In the model the starting location of the chassis COG has been

assumed coincident with the position where the *x* and *y* of the ground reference system are null, namely right above the inertial reference system origin. The starting height of the COG is 0,3m above the ground, as for the 2708RR car.

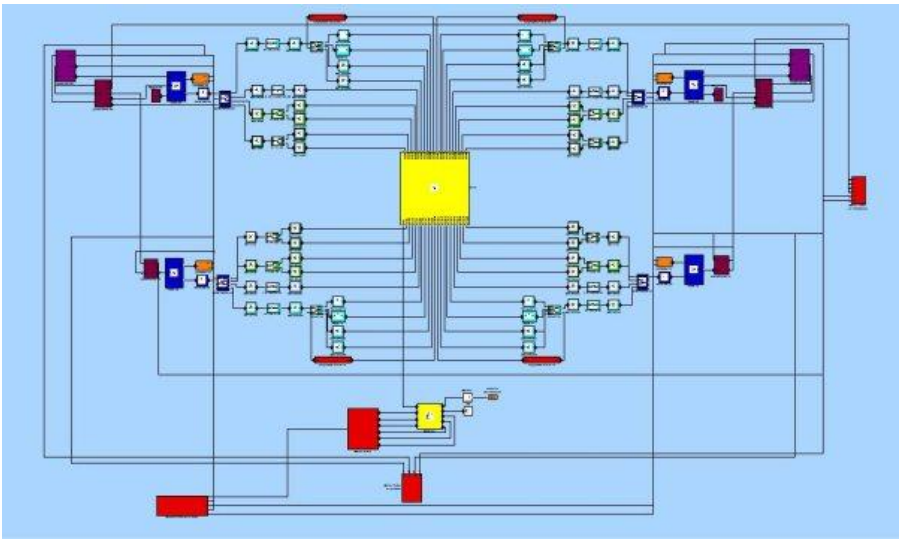

Figure 4.1 - Complete model

The block *Ground* needs to be connected to a *Machine Environment* block, in order to define the environment in which the system is working. This block, in particular, allows the simulation of the Earth gravitational attraction on the car and the setup of some simulating parameters (like the precision degree, the number of dimensions for the car visualization, etc.).

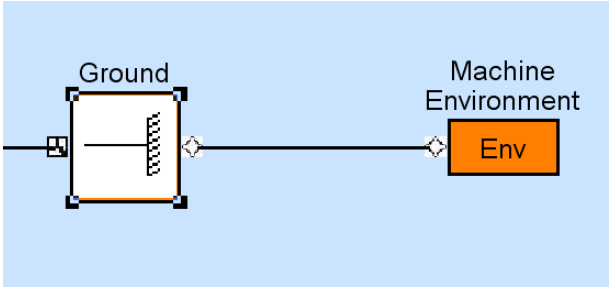

Figure 4.2 - Machine environment blocks

4.2.1 Chassis

The chassis has been modeled using a *Body* block (yellow colored) put in the middle of the model, as shown in Figure 4.3. This kind of blocks are able only to represent the mass and the inertia ellipsoid of a body; they are also able to associate to the same body different CS, specifying the origin location and the axis space orientation. In this schematization the *Body* block represents all the mass and inertia of the vehicle and the driver, with the exception of the suspensions and the wheels. Even if this is a hard assumption that cause a loss of precision, it permits a great simplification of the work, leading to appreciable results for the simulation.

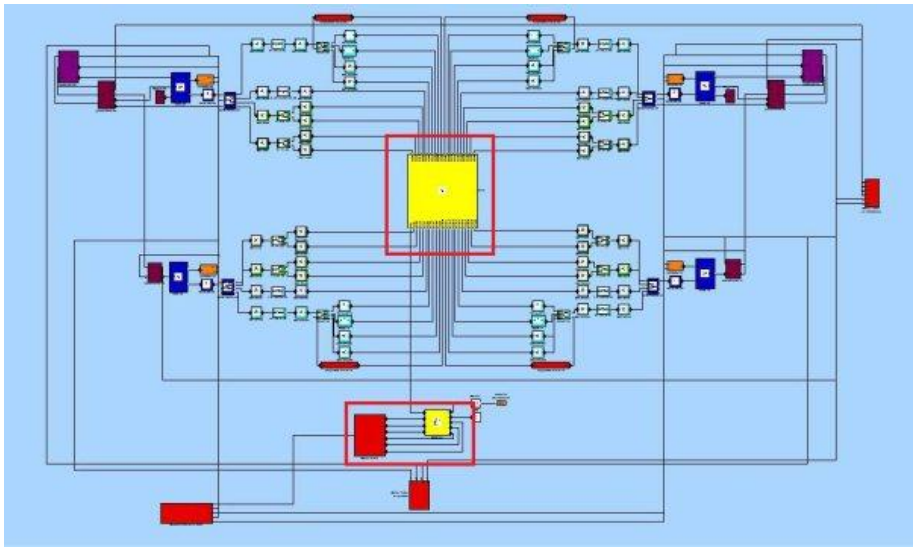

Figure 4.3 - Chassis blocks location

The *Body* block presents 32 Cartesian CS more than the COG's one. These CS have been defined and used to connect to the chassis all the other elements, like the suspensions; some others *ports* have been added to the chassis block, in order to connect to it some sensors and the four *Joints* representing the damper-spring group. The location of this points and their relative coordinates have been defined using the CAD model of the car, as the vehicle mass and all the inertia tensors of the body.

As shown in Figure 4.4, another block is related to the chassis: the *Custom Joint* (*CJ telaio* in the model). This block is used to model the relative DOF between two bodies. In this case it has been used, connecting the chassis to the ground, to model the relative DOF between the chassis and the Earth. As previously

said, the number of DOF is the maximum allowed, namely six. The *Custom Joint* block has also been used to specify the reference system that has to be used to study the motion, in this case the one on the ground. As is possible to note from Figure 4.4, this block is connected to another one, called *IC* (initial-conditions): all the initial conditions have been put equal to zero.

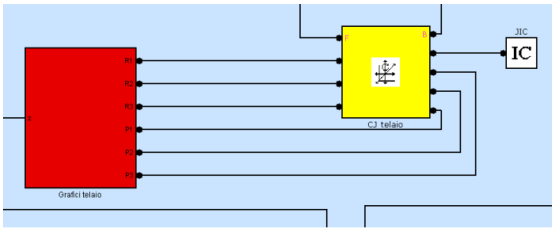

Figure 4.4 - Chassis *Custom Joint* and IC blocks

The *CJ* block is connected, using six ports, to a red block: this block contains six *Joint Sensors*, namely six blocks used to obtain the values of the components of the position, speed, acceleration of the COG, angular speed and acceleration, resultants of forces and moments in the COG, yaw, pitch and roll angles as a function of time. All these functions can now be plotted thanks to some *Scope* blocks, present inside the red block. As a matter of facts the red block, called *Grafici telaio*, is an hybrid one, containing both SimMechanics® and Simulink® parts, like the *Scopes*. All the kinematics dimensions are related to the inertial reference system.

4.2.2 Suspensions

The 2708RR car, like all the other Firenze Race Team cars, is equipped with a double wishbone suspension system: this kind of suspension is included in the group of the *independent* wheels, that is the one where the upright is connected to the chassis with a one DOF kinematic system. Double wishbone (DW) suspensions are composed by five elements: the upper arm, the lower arm, the steering track (or toe track for the rear wheels), the push (or pull) and the rocker.

All these elements, as shown in Figure 4.5, have been accurately represented in the model. To model this part of the vehicle four different SimMechanics® blocks have been used:

- *Body* blocks
- *Spherical joint* blocks
- *Revolute joint* blocks
- *Body spring and damper* blocks.

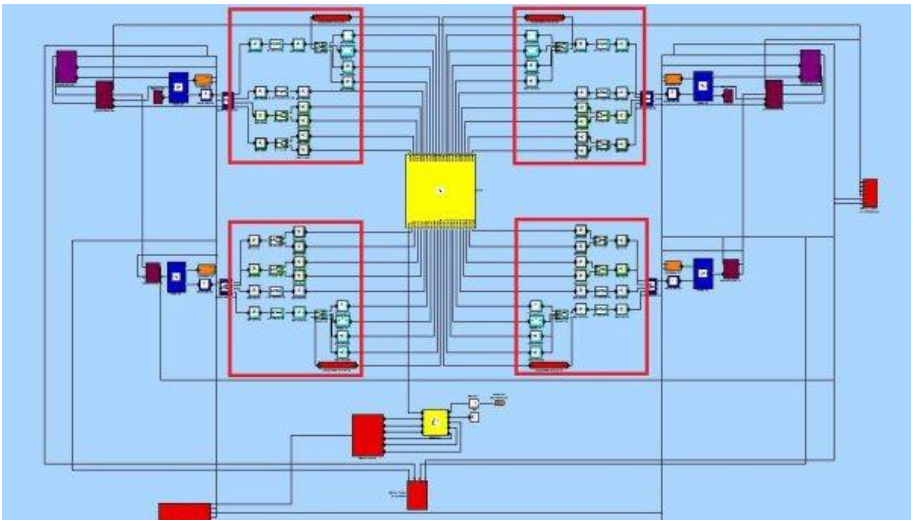

Figure 4.5 - Suspensions blocks

The *Body* blocks have been introduced previously and are used to represent a body, implementing its mass and inertia. These blocks have been used to model the upper and lower arms, the push and the rocker of all the four suspensions.

The *Spherical joint* are blocks representing effectively the spherical joints connecting two systems: they need two coordinate system coincident with the two bodies they connect.

The *Revolute joint* are joints that only allow a rotation to the body connected to the *F* port (*Follower*) among the body connected to the *B* port (*Base*). It's, of course, necessary to define the rotating axle for the body.

The *Body Spring and Damper* blocks represent the actions applied by the spring and the damper to the connected elements. Inside these blocks it's possible to define the initial length of the spring, its stiffness and the damping coefficient. As it's easy to imagine these blocks have to be put between two rigid bodies, side by side with the relative joints, as they do not possess any DOF themselves.

As is possible to observe in Figure 4.6, all these described joints have been put in the model in order to create a diagram representing the double wishbone suspensions configuration, proper of the Firenze Race Team cars. The *Body* blocks of the upper and lower arms have four Cartesian CS associated: one is the main CS, where the inertia ellipsoid is defined, one is coincident with the connection point between the arm and the upright and the other two are coincident with the connection points between the arm and the chassis. In this particular case the main CS has been hidden.

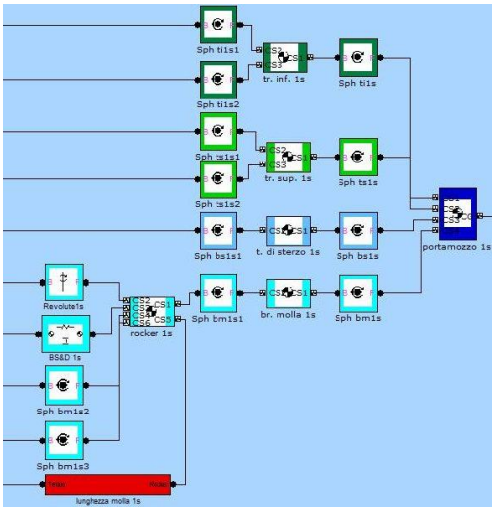

Figure 4.6 - Suspensions scheme

The coordinates of the COG of every arm and their inertial values have been obtained directly from the car CAD; the same for the coordinates of the connection points between the arms, the chassis and the upright. In particular the chassis and every arm have been connected using two *Spherical Joint*; these joints are not independent one from the other, as they consent to the arm a relative rotation around a straight line, connecting the attaching point of the arm itself to the chassis. On the other side of the arm there is another *Spherical Joint* that connects it to the upright. As the upright is connected to the other components by four spherical joints it has two DOF: one rotation around the steering axis and the vertical motion.

The steering tracks (or the toe tracks for the rear part) have been, again, modeled with *Body* blocks having three CS: the main CS with the mass and inertial data and the two used to define the connections with the upright and the chassis. All the connections have been schematized using the *Spherical Joint* element and the tracks have only one DOF, like the arms.

The water green parts are the one that schematize the push, the rocker and the damper-spring group. The pushrod has been modeled using a *Body* element with three CS. Even this block is connected to the rocker and to the upright using two *Spherical Joint* blocks.

The *Body* block representing the rocker has six CS associated, more than the main one. Three of them are used to connect the rocker with the spring, with the chassis and with the push, while two of them have been used to locate two *Spherical Joint* blocks, needed to represent the connections of the spring-damper element, as it has no internal DOF.

As is possible to note in Figure 4.6 there is another red block associated with suspensions, that is used to instantly calculate the length of the spring-damper group and to plot them as a function of time.

4.2.3 Wheels

The blocks modeling the wheels are the one represented, in Figure 4.7, in blue. Each single wheel has been modeled using three elements: two *Body* blocks and on *Revolute Joint* connecting them.

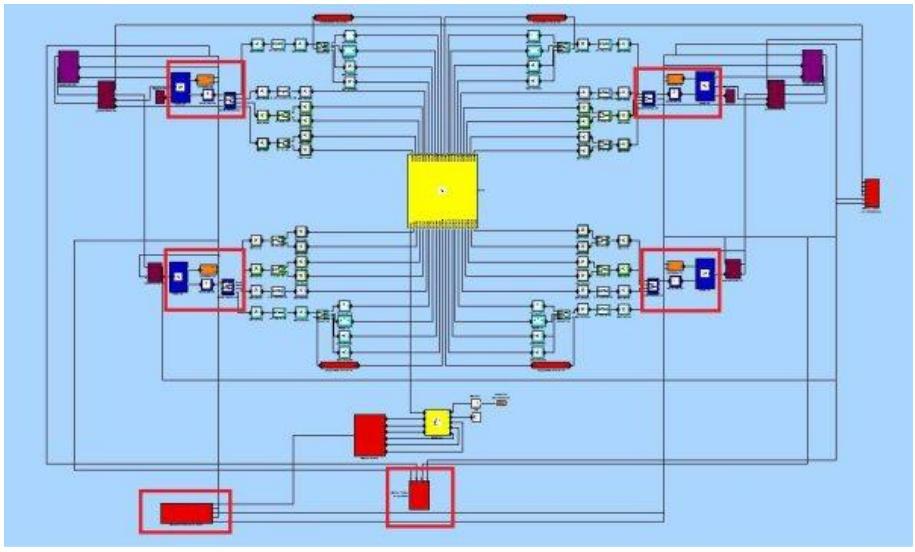

Figure 4.7 – Wheels blocks

The internal block represents the upright, whereto the suspension is attached. Every upright has the main CS with the mass and inertial characteristics, and four other CS where the arms, the tracks and the pushrod are attached. The rear wheels have also two more CS, needed to attach them to the actuation system. The block modeling the upright is connected to a *Revolute Joint* block that represents the DOF present between the wheel and the upright itself. This joint permits to the wheel the rotation around the *y* axis of the main CS of the upright. Due to the fact that the centers of mass of the wheel center and the upright differs only for the *y* coordinate, the transversal principal inertial axis of these two bodies coincides.

The wheel rim and the tyre have been modeled using a *Body* block, named *ruota*, that possess three or five ports, depending if it's a front or rear one.

For both of them the *CS1* port connects the wheel to the upright, the *CG* port (that is, effectively, the center of mass) is connected to the contact block, while the others are all coincident with the main CS and are used to connect *ruota* to the actuation.

The orange block connected to the wheel, shown in Figure 4.8, is used to model the road-tyre contact, practically defining the road plane.

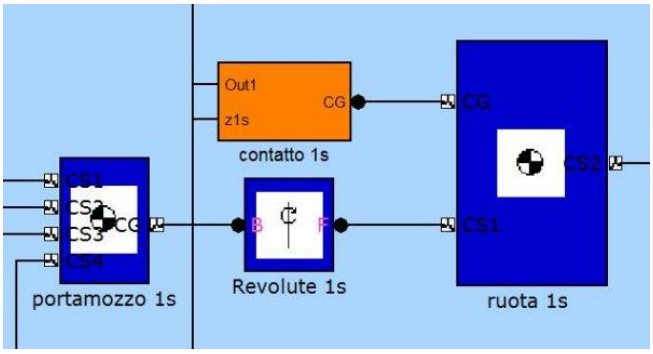

Figure 4.8 - Wheel block detail

The contact block measures, with a sensor, the position and the speed of the wheel center and compose two signal as column vectors. From the position a constant, the wheel radius, is subtracted in order to find the road-tyre contact point position, called δ. After this operation a dedicated block selects the only *z* component of the position and the signal is sent to a *if* cycle that has the duty to discern the negative signals from the positive or null; in other words it has to recognize if the contact point is going below the *x-y* plane of the CS associated to the *Ground* block. If the *z* coordinate results to be negative, the position vector is multiplied for a constant matrix (experimentally determined) and the obtained signal, that is again a vector, is applied as an elastic upward vertical force to the contact center. If the *z* component is positive or null, no force is applied, as no mutual penetration is present.

The speed is instead directly multiplied for a constant matrix and the signal, that became an upward vertical damping force vector, is added to the elastic force and applied to the wheel center.

The contact block also presents two exit ports: one of the output signal is merely the *z* component of the resultant of the elastic and damping force elaborated as above by the block. The so obtained scalar signal is plotted by a red block: the given graphs permit an easy visualization of the load difference between the wheels and the axles, that are requested to evaluate the vehicle turning behavior and its balancing.

From a strictly mathematical view the block models the following relations:

$$\begin{cases} \delta_{ij} = P_{gpij} - r \\ z_{gpij} < 0 \\ F_{zij} = K \cdot \delta_{ij} + B \cdot \nu_{gpij} \end{cases} \cup \begin{cases} F_{zij} = 0 \\ z_{gpij} \geq 0 \end{cases} \tag{4.1}$$

with $K, B \in \mathbb{R}$

The two constants *K* and *B*, are two matrixes having the only element x_{33} different from zero and negative, to be sure that the out coming block signal is effectively a column vector having the only vertical component different from zero and the vector modulus is positive.

Again there is another red block that measure the height difference between the chassis COG and the wheel centers, taken from the contact block. In this way it is possible to plot the wheel vertical travel.

4.2.4 Actuation system

The purple blocks in Figure 4.9 are the actuation ones that have the duty to apply the motor torque and the road-tyre interaction forces to the model.

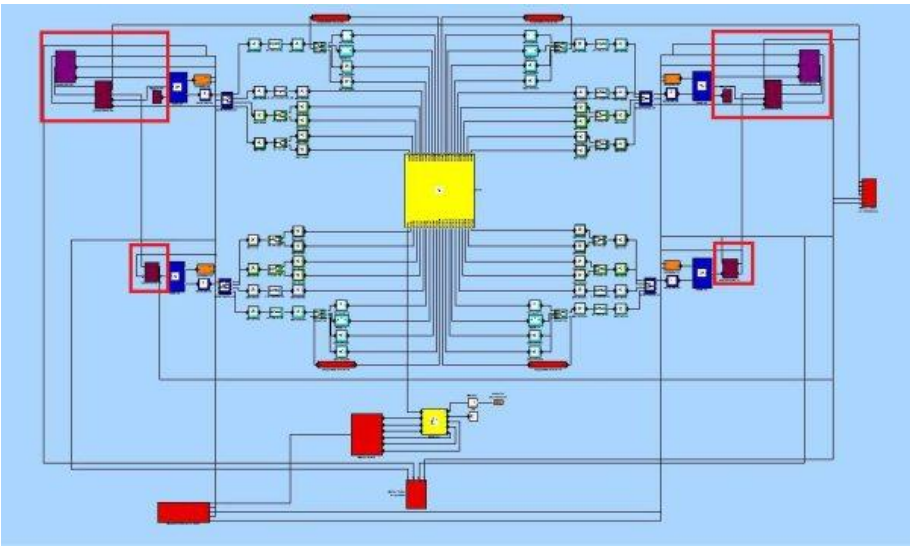

Figure 4.9 - Actuation system blocks

The two actuation system for front and rear tyres are different: the front tyre rolling is considered to be pure, while the rear tyres, being the driving ones, have their interaction forces calculated by some blocks that approximate the Pacejka model. The choice of using this different formulation for front and rear tyres, even if it's a hard simplification, permitted to really simplify the model and to avoid numerical errors shown during the tests.

The front tyre actuation block calculates the rolling torque starting from the force acting on the wheel center, coming from the driving wheels, and from the contact force, coming from the previously seen contact blocks.

The motor torque is generated by two identical blocks: they are directly connected to the rear wheel centers, and apply a momentum that put into rotation the wheel around the transversal axis. For the first simulation the torque starts from a value of 150Nm and increases up to 250Nm after five seconds.

The two rear wheels have two more blocks connected: they are a violet one, called *parametri*, and a purple one, called *pneumatico*.

The first one is used to calculate the slip angle and the longitudinal slip of each tyre, needed to define the entity of the interaction forces exchanged between tyre and road. Inside the *parametri* block there are two sensors: one is connected to the wheel center and is used to calculate the angular velocity of the wheel while the other is connected to the upright COG and is used to determine the speed. As the upright is not rotating with the wheel and being the connecting torque with the hub ideal, it's reasonably to suppose that the upright speed is almost the same of the wheel center and can be used to calculate the slip angle and the longitudinal slip. The *parametri* block also receive a signal with the contact force of each tyre, as it is necessary to determine the value of the modulus of the road-tyre contact. Thanks to the way the contact has been modeled, during cornering, these blocks take into account the load transfers due to centrifugal force.

Inside the *parametri* block it was necessary to introduce two *if* cycles, one to calculate the slip angle and one to calculate the longitudinal slip. These cycles are used to resolve some ambiguities during the first phase of the vehicle motion, when all the starting conditions are equal to zero, as well as the motor torque.

The other block, the so called *pneumatic*o, receives as inputs the values of the slip angle, the longitudinal slip and the contact force coming from *parametri* and returns to the model the vectors of the road-tyre contact forces, both in longitudinal and lateral directions. The modulus of these forces are also sent to a red block that plots them as a function of time.

It has to be noticed that the interaction forces have to be applied in the contact point between road and tyres, however, during tyre rolling, every point of the tyre circumference could assume the contact position and SimMechanics® is not able to apply a force on a zone. It was so necessary to adopt a trick: the force is

always applied in the wheel center, adding to them some “transport moments”. In particular, the forces have been applied in the upright COG, as these points translate without rotating, while the transport moments have been applied to the wheel centers not to lose the torque generated by the longitudinal interaction forces that opposes to the motor torque that cause the front tyre rotation.

It has also to be noticed that this model does not perfectly model the road-tyre interaction forces, but approximate them with a function built ad-hoc.

For each tyre, the transversal interaction force with the ground is function of the slip angle, of the contact force and of the corresponding force in longitudinal direction, while this is function of the longitudinal slip, of the contact force and the interaction transversal force itself.

Let’s now analyze how the contact force has been modeled, using part of the experience of the Firenze Race Team. The starting point is a linear function, obtained by interpolation, that represents the transversal force of a generic tyre as a function of the slip angle and parameterized on three different values of the contact force. The nodes of this function have been inserted in a specific block that receives as input the slip angle and the contact force, coming from the *parametri* block, and that builds a first approach transversal force module function by means of approximation. This function, however, does not take into account the instantaneous value of the modulus of the longitudinal interaction force, acting on the same wheel. A second block is therefore been implemented, receiving as input the function as above and the signal of the same function but for the longitudinal direction. The block now builds a function of these two signals, still using linear interpolation, that approximates the contact ellipsis of the tyre and calculates the modulus of the transversal force that is now effectively applied to the upright COG.

With a perfectly analogue course the function over time of the longitudinal forces have been obtained.

4.3 Testing the model

Thanks to the outputs of the model, it's possible to plot some of the most interesting quantities to evaluate the strength of the model. These quantities are:

- the contact forces
- the dampers travel
- the resultant of forces and moments in the chassis COG
- the interaction forces
- The position, speed and acceleration of the chassis COG
- the chassis angular velocity
- the chassis angular acceleration
- the chassis yaw, pitch and roll angle.

It has to be remembered that SimMechanics® permits con connect any number of sensors to any body in the model, so the choice to plot these particular dimensions was completely arbitrary.

The model simulates the behavior of the vehicle supposing to accelerate it on a straight road with a starting engine torque of 150Nm. This acceleration will now linearly increase through the next five seconds, stabilizing at 250Nm, as shown in Figure 4.10.

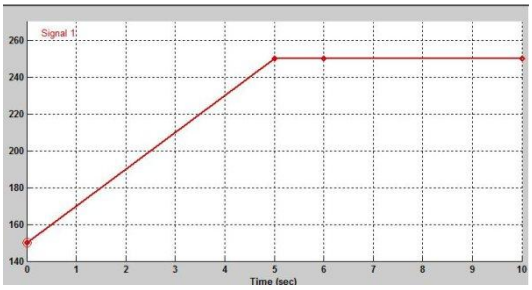

Figure 4.10 - Acceleration trend

The choice of starting the car with a non null torque is due to the way the longitudinal forces are applied to the wheels: the actuation blocks almost immediately start to generate a longitudinal interaction force between the road and the tyre and, with this, the relative torque that oppose to rolling. Due to the fact that internal friction is neglected, if the initial engine torque is zero, a negative reaction force would be applied to the rear wheels, producing a wrong simulation of the motion.

4.3.1 Contact forces

The contact forces are the one that, ideally, the road surface applies on the wheels in vertical direction. These forces are a resultant of the of an elastic and a damping force and are function of the position and speed of the contact point. In this model the contact forces represent effectively the road ground, as SimMechanics® does not possess a specific block for this duty. It's possible to say that the vehicle "falls" until an equilibrium between the weight forces, generated by the *Machine Environment* block, and the contact forces is reached. This equilibrium is quickly reached and is not perceived by an observer. It has anyway to be noticed that the contact forces have an initial growing phase until stabilization; from now on, as shown in Figure 4.11, they remain almost constant, with the exception of some oscillations. In the block that regroups the signals of the contact forces there are three graphs.

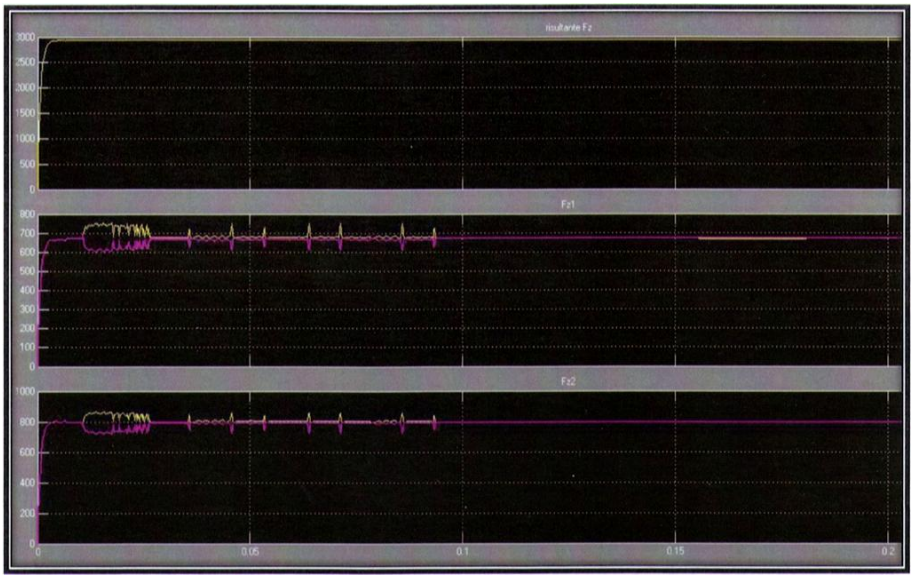

Figure 4.11 - Contact forces

The first one represents the sum of the forces on the four wheels; the resultant has an intensity equal to the sum of the four forces modulus, with vertical upwards direction. The second and third signal represent, respectively, the trend during time of the contact forces of the front and rear tyres. As it's possible to observe the resultant of these forces oscillates around the value of the total car weight modulus, that is 2940N.

Another note has to be made on the entity of the rear contact forces in comparison with the front ones: these are effectively larger. This fact is due to the longitudinal load transfer during acceleration, and to the increase of car weight on the longitudinal axis (due to the presence of the engine and the driver).

Due to the fact that this first test is made on a straight path, and the longitudinal load transfer is not neglectable, it seems to be interesting to comment it.

4.3.2 Wheel shake

The wheel vertical travel is given, instantly, by the height difference between the chassis COG and the wheel centers:

$$Z_{gT} - Z_{gRij} \tag{4.2}$$

The calculation of these functions is really useful to observe the longitudinal load transfers during motion and assumes a particular meaning when it is related to sudden accelerations, like during turning.

A first indication on the model proper response can be found in the wheels travel. The front wheel travel has to be smaller of the rear wheels because, when the vehicle accelerates, the system inertia let the chassis “move” to the back axle, generating the elongation of the front spring-damper group and the contraction of the rear one, corresponding to a decrease and an increase, respectively, of the height difference between the chassis COG and the analyzed wheel center.

It has to be remembered that the chassis COG is initially located at 300mm above the ground while the wheel centers are at 254mm from the ground. The road has been modeled without any asperity (but it’s possible to model almost every kind of ground, with no limitations).

Let’s now analyze the graphs of the introduced dimensions. The block that receives the signals of the wheel travel has two *Scope*, that includes two different graphs: the first represents the front wheels travel, left and right, while the second the rear ones, in the same order. Observing Figure 4.12 it’s possible to note that the front wheel travel decreases; this means that the chassis COG tends to reduce its height, like the front tyre centers, but their height difference decrease step by step during simulation because the wheel centers height reduction results to be lower than the chassis COG, due to the longitudinal load transfer.

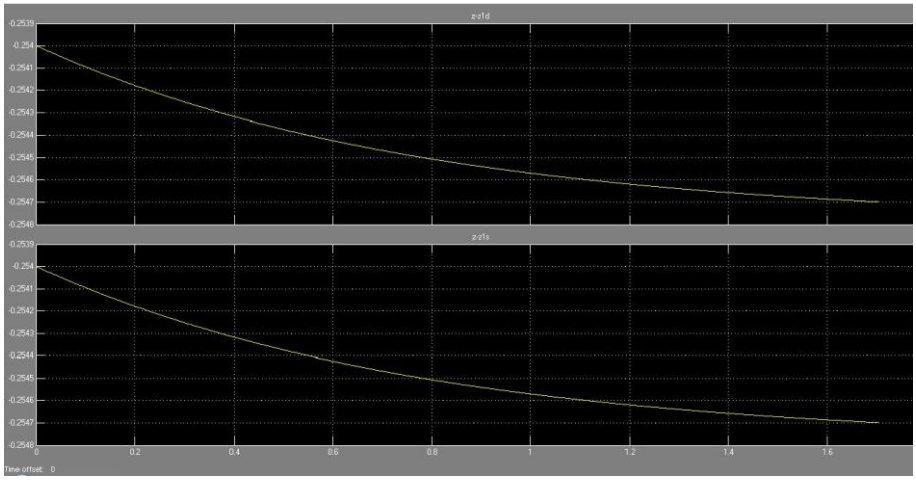

Figure 4.12 - Front wheels travel

For what concerns rear wheels, as shown in Figure 4.13, their trend is decreasing. The height decrease of the rear wheels is however larger than the chassis COG, generating and increase between these two heights.

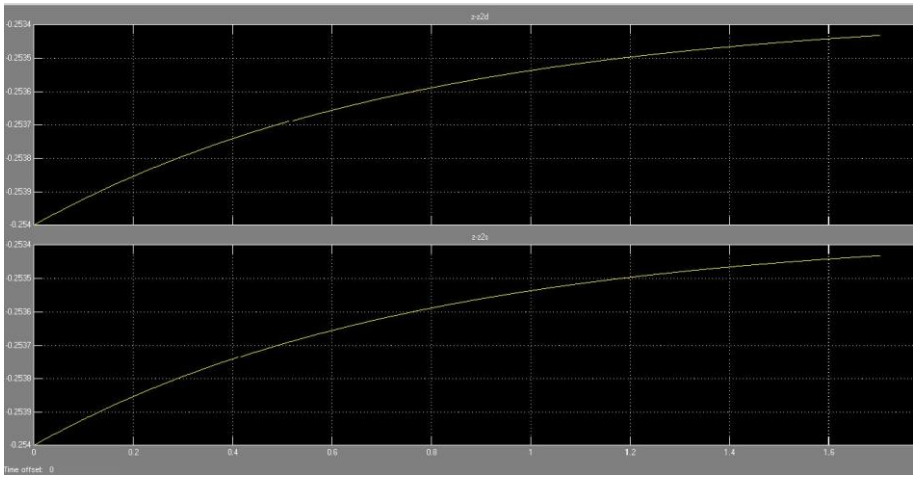

Figure 4.13 - Rear wheels travel

As the model is moving on a straight path, the wheels on the same axle have the same vertical travel, with only some small differences, due to little numerical errors.

4.3.3 Test results

This simple test is, however, significant for what concern the analysis of the model response. Even if some great simplifications have been introduced in the model, the vehicle seems to pretty well respond to the acceleration imposed and gives results well aligned with what was expected and what could be easily calculated with other commercial programs. Wheel travels and chassis motions are perfectly compatible with the maneuvers imposed, and the same for the COG position, speed and acceleration, as shown in Figure 4.14.

As previously seen the contact forces are well plotted and seems to be in line with the way the block is modeled and to what we expected. The great advantage of the model is the way the "road" is modeled, using the contact forces to instantly reproduce the interactions between road and tyres: as we verified the proper response of this interaction, we're now sure that its use is an advantage and let us reproduce, in case, even a "poster rig" function, effectively shacking each tyre as preferred.

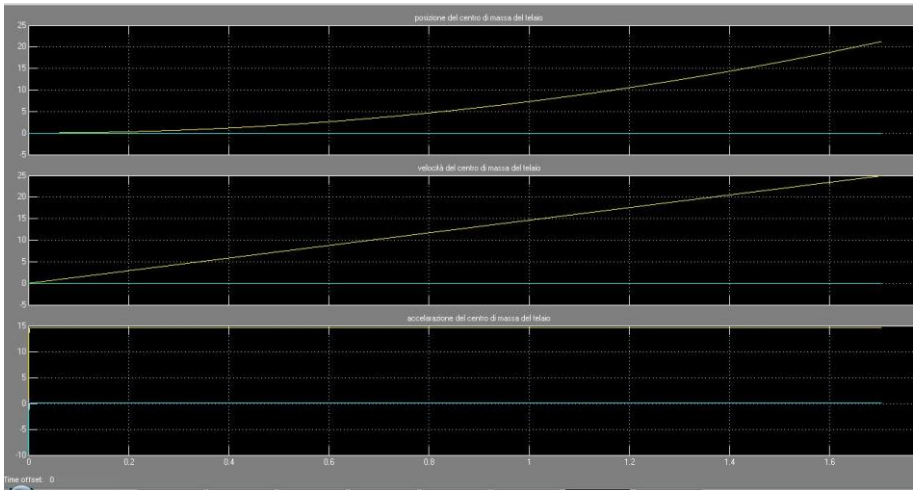

Figure 4.14 - Position, speed and acceleration of the COG

It's now time to further test the vehicle model on a much more difficult test, confronting it with a commercial software like MSC.Adams®.

4.4 Model comparison: skid-pad test

During the last year the Firenze Race Team approached the problem of vehicle dynamics analysis using a commercial software, Adams Car®. With this software it was possible to build a model of the various Formula SAE cars, i.e. the 2708RR [10], starting from some pre-existing templates and modifying them to fit the different cars configurations. After some years of experience with this software, it was decided to start the construction of a self made model, that originally born on one of the team's car and is easy to adapt to these cars. Of course the gaining of sensibility on vehicle dynamics through the last years gave a great help to the development of this vehicle model, but is not sufficient to prove the effective functioning of it. It was so decided to test the new model on a common maneuver with Adams Car®. The selected maneuver is a common skid-pad, as the one shown in Figure 4.15.

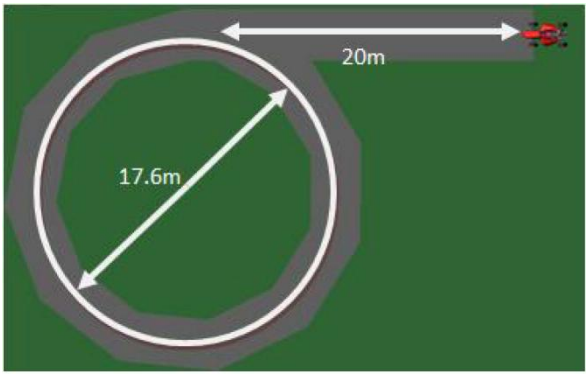

Figure 4.15 - Skid-pad test

Differently from the skid-pad of the chapter 3.4.1, this is a single lap one, as we already had it implemented in Adams Car® environment. The turn radius remains the same of the Formula SAE rules, 8,8m. The car travels a straight 20m line, than starts to turn: the first straight part is needed in order to let the SimMechanics® model find its equilibrium. Both vehicles (the "Adams Car®" one and the SimMechanics® one) faces the test having the same speed of 10,4m/s that produce, during turning, a lateral acceleration of 1,25g. This values has been chosen as it's the average lateral acceleration recorded by the 2708RR telemetry during the real skid-pad test.

Both cars have been set up with the same parameters for spring and dampers and have been subjected to the same starting conditions. Of course the way the models represent the test is not the same, as is not the same the

mathematical way they resolve the equations of the system. It's so easy to predict that some differences could manifest during the comparison.

Figure 4.16 shows the imposed dampers force-to-speed curve. For both models it has been used the same, even, of course, it has been built in different ways for the two simulating environments.

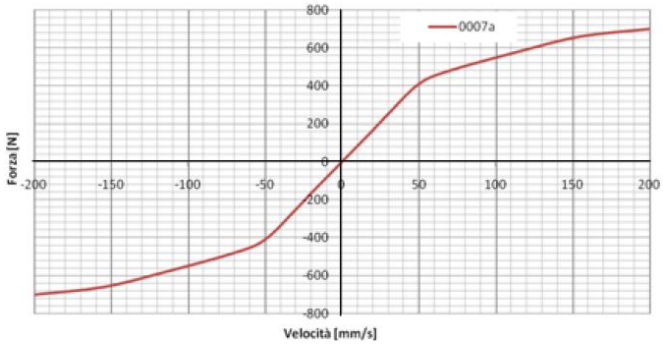

Figure 4.16 - Dampers force-to-speed curve

Once the two models have performed the required operations and maneuvers it was possible to export some of the most interesting comparison data and plot together, using Matlab®.

It has to be noticed that, for the Firenze Race Team (briefly called FRT in the next pages) model it was necessary to introduce a filter on the received output signal, as the particular way the model itself has been built, produces very dirty signals. Anyway, after having scaled and adapted the signals to the plot, it was possible to analyze the behavior of the two "cars" and compare them.

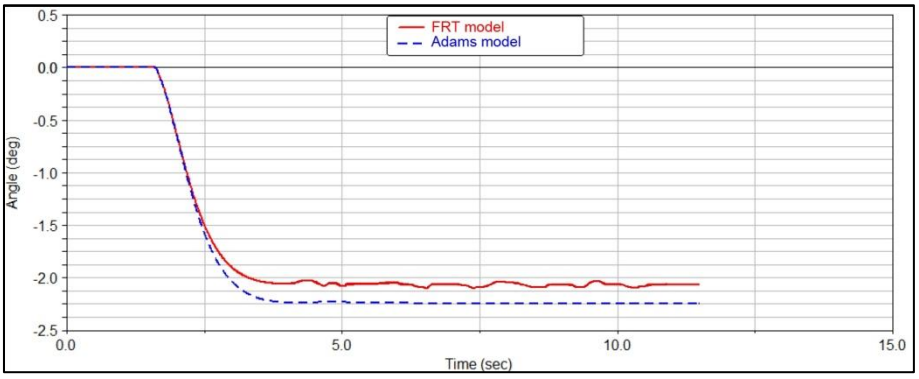

Figure 4.17 - Roll angle comparison

The first result that has an interest is the roll angle that the car has during the run, as shown in Figure 4.17.

As it's possible to note the two models show the same trend for this quantity, even if they are not properly the same. The Adams® model has a much more regular behavior, reaching the steady state during the corner covering, while the FRT model still presents some oscillations during the whole turning. This problem is probably due to the actuation system, that constantly applies its forces on tyres, or to the way the steering is managed, namely applying lateral forces on road-tyre contact point.

Figure 4.18 shows the behavior of the front external spring length during the whole test: again the two models, that have been set up with the same parameters, manifest the same behavior, differing one from the other for a small quantity, with an error less than 8%.

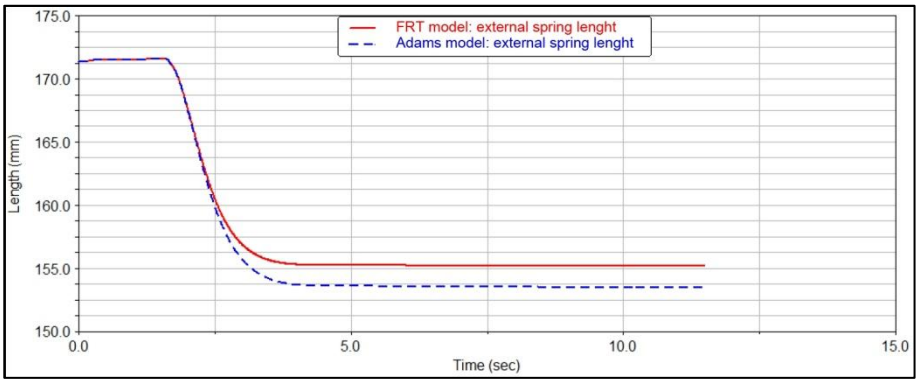

Figure 4.18 - External spring length comparison

Another interesting parameter to compare the two models is the slip angles of the two external wheels, shown in Figure 4.19. Again the trend of the two systems is almost the same, even if the FRT model shows a smaller difference between front and rear wheel. This is probably due to the way the FRT model has been built for what concerns slip angles calculation: ideal joints, friction absence and, maybe, some approximations led to the born of these differences that are, anyway, small enough and do not sensibly modify the behavior of the car on track.

The last, but really important, parameter shown is the one of Figure 4., the lateral load transfers on internal tyres, both front and rear. Again the FRT model perfectly respond to the test, aligning its results to the one of the more robust and tested Adams Car®, showing a difference in order of 10%. It has to be noticed again that the FRT model outputs have been strongly filtered to avoid excessive oscillations of the signal thus making impossible a comparison with the other data.

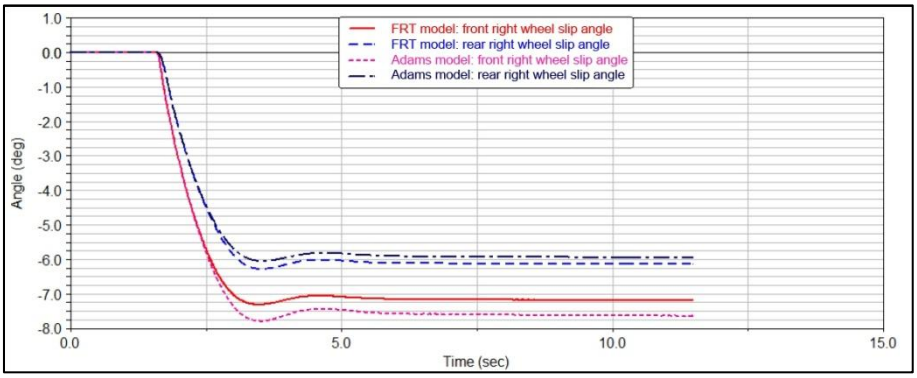

Figure 4.19 - Wheels slip angles

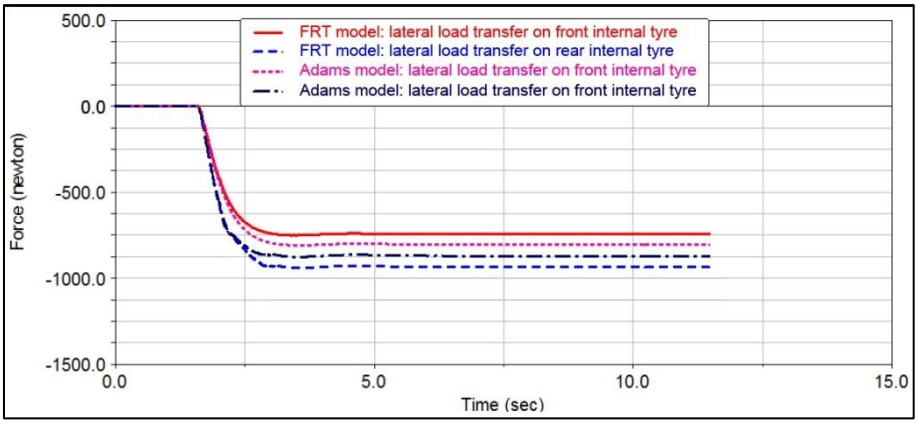

Figure 4.ù - Lateral load transfers

4.4.1 Comments on results

As shown the FRT model greatly respond to the simulation inputs, granting some good results for the main parameters needed to study the vehicle dynamics. All the differences between the MSC.Adams Car® model are contained and never exceed the 10%, thus granting robust results. It's interesting to note how the FRT model has been directly built on the Firenze Race Team cars, using all the real parameters and modeling each component to perfectly fit to the real ones installed on board. Of course this could be a great advantage in case this tool is used only inside the team, as all the modifications to fit new year's cars would be fast and much more robust. On the other hand, using the model with different kind

of vehicles could result in a prohibitive task, as all the internal schematizations have to be modified to adapt, for instance, to different suspensions geometry or driving wheels configurations. On this aspect, a software like Adams, is much more appreciable as, with the logic of its templates, it could fast and easily fit to different car configurations.

The self built model has some interesting features that grant it to be a really useful tool for the team. First of all, due to the way it has been built, it perfectly fits to any Formula SAE car, effectively modeling all the main parts and giving the user a completely free interaction with it (provided he has some knowledge of the Simulink® interface).

Another great advantage of the model is its capability to function as a direct dynamic simulator or as a static "poster rig", effectively simulating chassis response to road solicitations: this capability is given by the way the road-tyre contact has been modeled, namely applying forces in the contact point and equilibrating them with weight and load transfers. The poster-rig feature is really useful to test the chassis and suspensions response to road solicitations on any different situation it could be rebuilt starting from car telemetry. Acquiring dampers potentiometers signals and combining them together with the data from the inertial cell (that registers the lateral, longitudinal, vertical and angular acceleration of the vehicle) it's possible to reproduce every racetrack the car has traveled, effectively working and simulating the vehicle setup.

5 Conclusions and final remarks

In the world of competitive motorsport the aim of every team and, thus, engineer, is to design a fast and competitive car. To do so, more than a lot of experience and basic theory, it's necessary to use the right tools, in order to maximize the effort and minimize the time spent in designing and, after, eventually correcting setup errors on track. It's also a must to note that, when the car is ready and starts its life on race grounds, it would probably need many hours of testing to find the proper setup for every track it's called to run on. Many hours of testing correspond to a lot of money and time spent. It's so easy to understand how the use of a proper tool that could assist the designer during the whole designing process, giving direct indications of the possible car response on track, could be a great advantage.

Starting from the first part of this work, it was decided to deeply analyze the dynamic of a race car, acquiring the needed know-how and sensibility to start working on the mathematical models of a formula car, namely a Formula SAE one. The first part so focuses its attention on the various vehicle models that could be found in literature, in order to study the bases for the future implementation of the mathematical model.

After a review of the basic concepts of vehicle dynamics and handling a first model has been presented. This is a 3 degrees of freedom model, modeled in Simulink®, that has firstly been used to study a very easy vehicle motion. The model has been implemented to easily model almost all the maneuvers the car could do, like simple step-steers and skid-pads. Thanks to the fact that the whole model has been built directly using the last Firenze Race Team car, it perfectly simulates this vehicle behavior, as it has been proved during the simulations, confronting both experimental and mathematical results. The 3DOF model has been implemented especially for what concerns the driveline, modeling the different kind of differentials (open, rigid and LSD) and has been used to study the influence of this element on the vehicle handling. The results of the tests to which the model has been subjected demonstrate how this perfectly simulates the real vehicle behavior (in particular during the steady state phase of the turn) and have been used to

study the setup of the car for some of the most important phases of a Formula SAE race.

In the second part of this work another model has been introduced: while the 3 DOF model was perfect to simulate the general car behavior in most cases, it had some internal lacks that let it be only a first step for the creation of a proper designing tool. The great stride of the whole work was the creation of the 15 DOF model; this new tool allowed a total car simulation, including suspensions, road-tyre contact and a free possibility of configuration for it. Again this model has been built using all the geometric and inertial data of the real car, including dampers setup, springs and anti-roll bars stiffness. The basic idea of this model was to produce a tool able to easily and quickly adapt to any different Formula SAE car designed by the team, and capable of simulating its dynamic behavior in terms of accelerations (mainly lateral, longitudinal and yaw), characteristic angles (roll, pitch and yaw) and all the parameters needed to characterize a vehicle handling. Thanks to the way the model has been schematized it results to be easily adaptable to different configurations both for driveline, suspensions, engines and geometrical properties. As the interaction between road and tyres has been modeled using a particular characterization (namely directly modeling the interaction forces), the model also aid to be used as a poster-rig simulator.

To prove that the 15 DOF model could be used during the designing and setup phase of a Firenze Race Team car, it has been compared, in terms of results, with a well known and robust software: the results are perfectly comparable and proved that the model developed by the team almost perfectly simulates the behavior of the car on the most common maneuvers (i.e. an acceleration and a skid-pad).

List of figures

Bibliography

[1] M. Guiggiani, *Dinamica del veicolo*: CittàStudi edizioni, 2007.

[2] G. Genta, *Meccanica dell'autoveicolo*: Levrotto & Bella Editrice S.a.s., 1993.

[3] T. D. Gillespie, *Fundamentals of vehicle dynamics*: SAE International, 1992.

[4] W. F. Milliken and D. L. Milliken, *Race car vehicle dynamics*: SAE International, 1995.

[5] International Standard ISO 4138, "Road vehicles - Steady-state circualar test procedure", International Organization for Standardization, 1982.

[6] H. B. Pacejka, *Tire and vehicle dynamics*: Butterworth-Heinemann, 2002.

[7] G. Greco: Tesi di dottorato di ricerca - Università di Pisa, 2007, pp. 19-54.

[8] Milliken Research Associates. Formula SAE Tyre Test Consortium. [Online]. http://www.millikenresearch.com/fsaettc.html

[9] SAE Internationals, *Formula SAE rules*, 2009.

[10] J. Cecconi, *Analisi ed ottimizzazione della dinamica di una vettura Formula SAE*. Firenze: Tesi di laurea - Università degli Studi di Firenze, 2007/2008.

[11] H. Heisler, *Advanced vehicle technology*: SAE International, 2002.

[12] H. Huchtkoetter and T. Gassmann, *Vehicle dynamics and torque management devices*: SAE technical paper series, 2004.

[13] A. Morelli, *Progetto dell'autoveicolo. Concetti di base*: Celid, 2004.

[14] M. Pedrinelli and F. Cheli, *On the powertrain dynamics influence on vehicle performance: the differential*: SAE technical paper series, 2006.

[15] V. V. Vantsevich, *All-wheel driveline mechatronic systems: principles of wheel power management*: SAE technical paper series, 2006.

[16] T. Amato, F. Frendo, and M. Guiggiani, "Handling behavior of vehicles with locked differential system", in *FISITA*, Barcelona, 2004.

[17] D. Capra, N. D'Alfio, A. Morgando, and A. Vigliani, *Experimental test of vehicle longitudinal velocity and road friction estimation for ABS system*: SAE

International, 2009.

[18] A. Reim, A. Steinbach, O. Oettgen, and D. Stapel, *Central sideslip angle estimation on a software integration platform*: SAE International, 2009.

[19] W. Cho, J. Yoon, K. Yi, and T. Jeong, *An investigation into unified chassis control based on correlation with longitudinal/lateral tire force behavior*: SAE International, 2009.

[20] A. Sorniotti, *Driveline modeling, experimental validation and evaluation of the influence of the different parameters on the overall system dynamics*: SAE International, 2008.

[21] C. Ghike and T. Shim, *14 degree-of-freedom vehicle model for roll dynamics study*: SAE International, 2006.

[22] T. Amato, *Analisi del comportamento dinamico di veicoli dotati di differenziale*: Tesi di dottorato di ricerca - Università di Pisa, 2006.

[23] F. Cheli et al., "Development of a new control strategy for a semi-active differential for a high-performance vehicle", *Vehicle System Dynamics*, vol. 44, no. S1, pp. 202-215, 2006.

[24] N.K. M'sirdi, A. Rabhi, N. Zbiri, and Y. Delanne, "Vehicle-road interaction modelling for estimation of contact forces", *Vehicle System Dynamics*, vol. 43, no. 1, pp. 403-411, 2005.

[25] Y. Zhenhui, C. Mousseau, B.G. Kao, and E. Nikolaidis, "An efficient powertrain simulation model for vehicle performance", *International Journal of Vehicle Design* , vol. 47, pp. 189-214, 2008.

[26] A. Botrini, *Modello matematico di un veicolo Formula SAE*. Firenze: Tesi di laurea - Università degli Studi di Firenze, 2008/2009.